

STUDIES OF REGULATORY NETWORKS IN CELLS:

ROLES OF IONS AND SMALL MOLECULES

Thesis by

Neal Bruce Handly

In Partial Fulfillment of the Requirements

for the Degree of

Master of Science

California Institute of Technology

Pasadena, California

~~1985~~ 1984

(Submitted May 25, 1984)

Acknowledgements

I greatly appreciate the support and freedom to explore my own ideas that has been provided by my supervisor, Professor John Richards. I am also thankful for many discussions, both entertaining and educational, with Professor Richards, members of the group and others at Caltech. I have enjoyed and hope I will continue to enjoy the friendships of Brian Herndier, with whom much of the muscle work was developed and Rob Kaiser. Both were able to improve my attitude when all seemed impossible.

Scientifically, I would like to thank the following people who have contributed to this work: Dr. Jim Hudspeth, Barry Kuppermann, Larry Katz, Arthur and Kathy Talaro, Howard Kurasaki, Dr. Mike Stoll, Dr. Juana Acrivós and a special thankful memory to Dr. Bob Vaughan.

I shall not forget the hospitality of other departments when refreshments were served at their seminars; I even learned a few things about astrophysics.

I am grateful for financial assistance from the NIH, the Earle C. Anthony Fellowship and many other supplemental awards.

To all the others, my thanks and good wishes.

Chapter 1 Abstract

In frog skeletal muscle, verapamil behaves as a Ca^{+2} antagonist and promoter of Ca^{+2} release from the sarcoplasmic reticulum (SR) depending on the concentration of the drug. The regulation of Ca^{+2} metabolism by verapamil was examined in four ways.

1) A determination of the effects of verapamil on $^{45}\text{Ca}^{+2}$ uptake into artificial lipid vesicles and frog skeletal muscles was made. Verapamil was shown not to be a Ca^{+2} ionophore, however it does interact with muscle to enhance uptake of $^{45}\text{Ca}^{+2}$ into bound stores.

2) Muscle tension was measured after verapamil treatment under a number of pretreatment conditions. Verapamil was found to cause a dose dependent contracture that was independent of extracellular Ca^{+2} , was facilitated by an intact t-tubule system and was inhibited by dantrolene, which blocks the release of Ca^{+2} from the SR.

3) The membrane potential of frog skeletal muscle was monitored during verapamil exposure. No effect by drug treatment on potential was observed.

4) A study of $^{86}\text{Rb}^{+}$ efflux from muscle, an indirect measure of intracellular Ca^{+2} via Ca^{+2} - dependent K^{+} conductance, was performed with verapamil alone or with dantrolene pretreatments. At concentrations greater than 0.1 mM, verapamil inhibited $^{86}\text{Rb}^{+}$

efflux, however above 0.6 mM it enhances $^{86}\text{Rb}^+$ efflux by causing the release of Ca^{+2} from the SR.

Our work suggests an as yet uncharacterized antagonism of Ca^{+2} by verapamil (reducing Ca^{+2} at the inside of the membrane). At higher concentrations, verapamil acts on the SR or some portion of the t-tubule system to release Ca^{+2} from the SR and elevate intracellular Ca^{+2} to a level that can activate the myofibril apparatus and stimulate K^+ conductance.

These results are consistent with a two site model of the action of verapamil, one generally distributed on the plasmalemma where the drug either blocks Ca^{+2} entry or causes a reduction of $[\text{Ca}^{+2}]$ at the inside of the membrane by blocking some intracellular pool and a second site within the t-tubule or on the SR itself where the drug causes the release of SR Ca^{+2} . This latter site and interaction may be related to the process of excitation-contraction (E-C) coupling.

Chapter 2 Abstract

The mechanism of action of Compound 48/80 to control cytoplasmic Ca^{+2} in muscles has been explored. The drug was found to affect frog muscle in the following ways:

- 1) Compound 48/80 caused a contracture independent of extra-cellular Ca^{+2}
- 2) The contracture effected by the drug is inhibited by treating the muscle with neuraminidase before drug exposure
- 3) The contracture is caused by the release of Ca^{+2} from the sarcoplasmic reticulum (SR) and from membrane bound stores
- 4) Treatment with drug did not affect membrane potential
- 5) Contraction threshold was elevated by drug exposure

These results are discuss in the context of the problem of excitation-contraction (E-C) coupling.

Chapter 3 Abstract

The development of an intracellular Ca^{+2} sequestering activity is studied in the rat myoblast cell line, L8. Under defined conditions the cells can be induced to develop into myotubes. The following two points could be made about the two cell types.

- 1) Compound 48/80 could enhance the uptake of Ca^{+2} into bound stores in both myoblasts and myotubes.
- 2) The myotubes showed a ten-fold greater uptake of Ca^{+2} than the myoblasts in the presence or absence of the drug.

Implications about the development of the sarcoplasmic reticulum (SR) and the value of this cell line as a model system for development are discussed.

The effects of nafenopin on cell division in several different cultured cells were examined and comparisons were made to its actions in intact rat liver. Among these cells, nafenopin was found to:

- 1) inhibit cell division and DNA synthesis in HTC and P815 cells.
- 2) temporarily inhibit or slow down mitosis in Lysobacter enzymogenes and E. coli LS1 bacteria.
- 3) not affect general protein synthesis in HTC cells. However, drug exposure was found to inhibit the synthesis of three apparently unrelated enzymes, thymidine kinase, α -lytic protease and penicillinase (RTEM), in HTC cells, Lysobacter enzymogenes and E coli LS1, respectively.

These results are in a marked contrast with the observations of the effects of the drug in the intact liver (e.g. dramatic increases in DNA and protein synthesis and mitosis). A discussion of the growth response in liver emphasizes the importance of two different cell populations; the hepatocyte, which appears to sequester and deactivate the drug, and a hepatocyte stem cell, which is recruited to help deal with the metabolic overload caused by nafenopin.

Chapter 5 Abstract

Proton nuclear magnetic resonance was used to probe the environment of the intercalant molecule in $1T\text{-TaS}_2 (\text{NH}_3)_{2/3}$ and $1T\text{-TaS}_2 (\text{N}_2\text{H}_4)_{4/3}$, and specifically look for phase transitions associated with changes in superlattice geometry. We find that there is a phase transition at 245°K in intercalated octahedrally coordinated TaS_2 that can be described by the following unique properties:

- A. The resonance frequency for the intercalated molecules indicates that there are different magnetic environments in three temperature domains.
 1. There is only one resonance field for molecules in isotropic magnetic environments.
 2. The high and low temperature domains (I and III) have molecules in only two different environments, whereas in the middle temperature domain (II) there are at least four different magnetic environments.
- B. The different magnetic environments measured by the ratio of anisotropic to isotropic resonance absorption intensity (r_{ai}) indicate that:
 1. The ratios, r_{ai} 's, are constants of the sample in domains I and II.
 2. At low temperatures (domain III), r_{ai} depends on magnetic field polarization effects and temperature treatment of the sample.

- C. The different magnetic environments observed for ammonia and hydrazine appear to be determined by the host (1T/3R-TaS₂).

TABLE OF CONTENTS

Acknowledgements	ii
Abstracts	iii
Chapter 1	iii
Chapter 2	v
Chapter 3	vi
Chapter 4	vii
Chapter 5	viii
 Chapter 1: Verapamil: Ca^{+2} antagonist and activator of the release of Ca^{+2} from sarcoplasmic reticulum	 1
Introduction	2
Methods	4
Measurements of Ca^{+2} flux into artificial lipid vesicles	4
Intracellular recording	5
Assay of $^{45}\text{Ca}^{+2}$ uptake into bound stores	6
Measurement of $^{86}\text{Rb}^{+}$ efflux from muscles	6
Measurement of force of contracture	7
Results	8
Treatment of muscles with verapamil causes a contracture	8
Extracellular Ca^{+2} is not required for the contracture caused by verapamil	8
Effect of dantrolene on the contracture caused by verapamil	8
Effect of verapamil on muscles treated with hyperosmotic glycerol	13
Verapamil does not facilitate the transmembrane flux of Ca^{+2} or Rb^{+} through artificial vesicles	13
Effect of verapamil on Rb^{+} efflux from muscle	13
Uptake of $^{45}\text{Ca}^{+2}$ in muscle bound stores is enhanced by verapamil at high concentrations	16
Discussion	21
References	25
 Chapter 2: Control of Ca^{+2} in muscles by Compound 48/80	 27
Introduction	28
Methods	29
Neuraminidase treatment	29

Measurement of excitation threshold	29
Measurement of force generated by the muscles when treated with Compound 48/80	30
Measurement of Ca^{+2} flux into artificial vesicles	30
Results	31
Compound 48/80 causes a contracture in the presence or absence of extracellular Ca^{+2}	31
Neuraminidase treatment of muscle prevents the Compound 48/80 induced contracture	31
Dantrolene inhibits the Compound 48/80 induced contracture in Ca^{+2} free media	31
Contraction threshold is elevated by treatment with Compound 48/80	36
Compound 48/80 interacts with lipid vesicles to enhance transmembrane flux of Ca^{+2}	36
Compound 48/80 does not affect membrane potential in frog muscle	36
Discussion	39
References	45
 Chapter 3: The development of sarcoplasmic reticulum in muscle cell culture	 46
Introduction	47
Methods	49
Cells	49
Assay of $^{45}\text{Ca}^{+2}$ uptake into bound stores	49
Results	50
Calcium uptake into bound stores	50
Discussion	55
References	57
 Chapter 4: Studies of the mechanism of nafenopin	 58
Introduction	59
Methods	62
HTC cells	62
P815 cells	62
<u>Lysobacter enzymogenes</u>	63
<u>E. coli</u> containing pBR322	63

Assay of DNA synthesis	63
Determination of thymidine metabolism	64
Measurement of protein synthesis	64
Determination of total protein (Lowry)	65
Assay for a serum factor after nafenopin feeding that could stimulate growth	65
Measurement of penicillinase activity	66
Assay for α -lytic protease	66
Synthesis of $[^{14}\text{C}]$ nafenopin	67
Results	71
Nafenopin inhibits DNA synthesis and cell division in cultured mammalian cells	71
Effect of nafenopin on thymidine metabolism	71
Nafenopin inhibits bacterial growth and specific protein synthesis	71
Determination of the distribution of nafenopin in rats and HTC cells	71
Serum from nafenopin fed rats does not induce DNA synthesis in serum starved HTC cells	78
Nafenopin does not inhibit protein synthesis in HTC cells	78
Discussion	85
References	90
 Chapter 5: NMR study of $1\text{T-TaS}_2 \cdot (\text{NH}_3)_{2/3}$ and $1\text{T-TaS}_2 \cdot (\text{N}_2\text{H}_4)_{4/3}$	 91
Introduction	92
Methods	98
Samples	98
Intercalation	98
NMR spectroscopy	98
Results	100
Domain I 250-300°K	100
Domain II 245-250°K	107
Domain III 200-245°K	107
Discussion	111
References	115

LIST OF FIGURES

Figure number	Title	Page
1-1	Verapamil causes a contracture in muscles	10
1-2	Extracellular Ca^{+2} is not required for the verapamil induced contracture	12
1-3	Effect of dantrolene on the verapamil contracture	14
1-4	$^{86}\text{Rb}^{+}$ efflux shows a biphasic response when muscles are treated with verapamil	18
1-5	Verapamil enhances uptake of Ca^{+2} into muscle bound stores	20
2-1	Extracellular Ca^{+2} is not necessary for the contracture caused by Compound 48/80	33
2-2	Neuraminidase treatment inhibits the contracture caused by Compound 48/80	35
2-3	Dantrolene inhibits the Compound 48/80 contracture in the absence of extracellular Ca^{+2}	38
2-4	Model for the action of Compound 48/80	41
3-1a	Compound 48/80 enhances Ca^{+2} uptake in L8 myoblasts	52
3-1b	Compound 48/80 enhances Ca^{+2} uptake in L8 myotubes	54
4-1	Nafenopin inhibits DNA synthesis in HTC and P815 cells	73
4-2	Effect of nafenopin on growth of <u>Lysobacter enzymogenes</u>	77
4-3a	Growth of <u>E. coli</u> LS1 in the presence of nafenopin	82
4-3b	Effect of nafenopin on penicillinase activity	84

Figure number	Title	Page
5-1	Crystal polytypes of TaS_2	95
5-2	Properties of hydrazine intercalated 1T- TaS_2	97
5-3	Orientational dependence of the separation between the anisotropic and isotropic resonance lines	104
5-4	Representative spectra for 1T- $\text{TaS}_2 \cdot (\text{NH}_3)_{2/3}$ at 300°K and 250°K	106
5-5	Effect of rotation on r_{ai}	110

LIST OF TABLES

Table	Title	Page
4-I	The effect of nafenopin on thymidine metabolism	75
4-II	The effect of nafenopin on α -lytic protease activity	80
4-III	Subcellular destribution of nafenopin in liver and HTC cells	87
5-I	Maximum separations in Hertz between the anisotropic and isotropic resonance lines	102

Chapter 1

Verapamil:

Ca^{+2} antagonist and

sarcoplasmic reticulum

activator

Introduction

In muscle, the regulation of a complex net of behavior is linked to the concentration of Ca^{+2} in the cell. Energy metabolism (Rasmussen, 1981; Hansford and Chappell, J, 1967), membrane transport (Bihler, I, 1972; Schudt, etal, 1976) and contraction (Caputo, 1978; Rasmussen, 1981) have been found to be modulated by variations of the same magnitudes of Ca^{+2} . The specific function of muscle is to receive electrical stimulation and respond with a contraction. When the stimulus is removed, it must return to a relaxed state. To achieve this cycle, the muscle modulates cytoplasmic Ca^{+2} between 5×10^{-8} M at rest and $2-3 \times 10^{-6}$ M at maximum contraction (Caputo, 1978; Rasmussen, 1981). At any given time in skeletal muscle, Ca^{+2} is determined by the release of Ca^{+2} from the SR into the cytoplasm and a reduction of cytoplasmic Ca^{+2} by Ca^{+2} -ATPases that sequester Ca^{+2} in the SR, mitochondria or send it outside the cell (Hasselbach, 1980; Hasselbach and Makinose, 1961; Ebashi, 1961; Ebashi and Lipmann, 1962). While the activities of the Ca^{+2} -ATPases that lead to muscle relaxation are fairly well understood, it is still not known how an electrical event (at the membrane of the t-tubule) initiates the release of Ca^{+2} from the SR to generate a contraction. This latter process is called excitation-contraction (E-C) coupling.

To understand the E-C coupling process, it is important to identify the subcellular structures that translate the muscle action potential into the release of Ca^{+2} from the SR and define

their function. Frank (1979) has proposed that Ca^{+2} ions associated with the t-tubule are mobilized by the action potential and these ions cause the SR to release Ca^{+2} thereby greatly amplifying the signal. Because of the similarities of chemical structure between verapamil, considered to be a Ca^{+2} antagonist (Fleckenstein, 1974; Cronin, 1982; Church and Zsoter, 1980) and Compound 48/80, which is a potent releaser of histamine from mast cells and which causes a contracture in frog muscle (to be published), an impetus was given to studying the activity of verapamil in skeletal muscle and to help complete our knowledge of the E-C coupling process.

Methods

Chemicals

Verapamil (Isoptin) was a gift of A. Knoll Pharmaceuticals, Whippany, New Jersey. Dantrolene was a gift of Norwich-Eaton Pharmaceuticals, Norwich, New York.

Frogs and muscles

Frogs (*Rana pipiens*) were obtained from Carolina Biological Supply. The frogs were double-pithed and skin was removed from the legs. The exposed muscles were bathed in oxygenated Ringers buffer: NaCl 6.78 g/l, KCl 0.18 g/l, MgCl₂ 0.4 g/l, tris (hydroxymethyl)-aminomethane 1.21 g/l, glucose 1.8 g/l and CaCl₂ 0.26 g/l (titrated to pH 7.2 with HCl): and care was taken to remove the muscles without damaging the muscle capsule. For most studies sartorius, semitendinosus, semimembranosus, gracilis major, gastrocnemius and an unseparated complex of peroneus, tibialis articus and tibialis posticus (shin complex) were used. Controls and treated muscles were made up of sets of similar size and the same type of muscle.

Measurement of Ca⁺² flux into artificial lipid vesicles

Artificial bilayer vesicles were prepared with L- α -phosphatidyl choline (Sigma). The CHCl₃ was removed under vacuum and a suspension of 5 mg/ml of the lipid was

made in EGTA-PBS (ethylene glycol bis (β -amino ethyl ether) N,N'-tetra acetic acid 38 mg/ml and sodium azide 0.02 g/l dissolved in a phosphate buffered saline (PBS): NaCl 8.0 g/l, NaHPO_4 1.15 g/l, KCl 0.2 g/l, KH_2PO_4 0.2 g/l). The suspension was sonicated on ice for 20 minutes at the 50% duty cycle setting and the 7 power setting with a Ultrasonics, Inc. sonicator model W-225R using the microtip. The vesicles were separated from the free EGTA by elution through a Sephadex (Pharmacia) G-50 column (0.8 x 35 cm) with PBS containing 0.2% NaN_3 and the light scattering peak at the void volume was collected. Vesicles (250 μl) were added to a reaction mixture of 1.5 μCi $^{45}\text{Ca}^{+2}$ (25 μl) and 100 μl of drug in PBS. At 5 and 25 minutes, vesicle-trapped $^{45}\text{Ca}^{+2}$ was separated from the free $^{45}\text{Ca}^{+2}$ in mini-columns of Sephadex G-50 as used by Levinson, etal(1979). (They were centrifuged for 1 minute at 2000 rpm in a Sorvall GLC-2 centrifuge.) The entire eluate was analyzed by liquid scintillation counting.

For studies of verapamil as a Rb^+ ionophore a similar protocol was followed except that EGTA was omitted in the vesicle formation step and vesicles were incubated with 1 μCi $^{86}\text{Rb}^+$ instead of $^{45}\text{Ca}^{+2}$.

Intracellular recording in sartorius muscle

Recordings were made with 15 M glass micro-electrodes filled with 3 M KCl and was connected to a WP Instruments DAM-5A amplifier. Sartorius muscles were pinned in

oxygenated Ringer's buffer and set up in Helmholtz cages. Five fibers were measured for each drug exposure for 15 minutes recording duration minimum. At 3.5mM verapamil exposure, recording was continued for 1.5 hours.

Assay of $^{45}\text{Ca}^{+2}$ uptake into bound stores

Excised muscles were exposed to various concentrations of verapamil in the presence of $0.5 \mu\text{Ci/ml } ^{45}\text{Ca}^{+2}$ in 2 ml normal Ringer's buffer. After 5 minutes incubation time, the muscles were removed from the labelled media, rinsed, and allowed to equilibrate 4 times for 30 minutes with fresh Ringer's as in the method of Bianchi and Shanes (1959). Muscles were then digested with 1N HNO_3 at 100°C for 20 minutes and aliquots were removed for scintillation counting.

Measurement of $^{86}\text{Rb}^+$ efflux from muscles

Muscles were incubated with $10 \mu\text{Ci/ml}$ of $^{86}\text{Rb}^+$ in PAB (NaCl 6.78 g/l, KCl 0.186 g/l, CaCl_2 0.199 g/l, MgCl_2 0.190 g/l, tris (hydroxymethyl) aminomethane 1.21 g/l, glucose 3.24 g/l, isoleucine 0.131 g/l, leucine 0.131 g/l, valine 0.117 g/l and insulin 10 units/l) for 1.5 hours at 25°C . The muscles were then washed several times with PAB to remove loosely associated surface Rb^+ . One half of the muscles were placed in $60 \mu\text{M}$ dantrolene in PAB, while the other half were transferred to normal PAB. After 20 minutes, muscles were then placed in tubes with drug and PAB with or without dantrolene and periodically aliquots of the

medium were taken for liquid scintillation counting. Total $^{86}\text{Rb}^+$ loaded into each muscle was determined by adding up amounts of each aliquot and the amount in a hot IN NaOH digest of the muscle.

Measurement of force of contracture

After surgical removal and any treatments with drugs or osmotic shock, the muscles were fitted into a Combielectrode (Katek Co.) equipped with an extracellular stimulating electrode and oxygen bubbler (provided with courtesy by A. Talaro) with 4-0 surgical silk so that the muscle lengths were 100-105% of normal rest lengths. A statham UC-3 transducer delivered force data to a polygraph and a Grass SD-9 stimulator was used to deliver electrical pulses to the muscle to test contractile response. A linear response curve was found between 50 mg and 3 g.

Results

Treatment of muscles with verapamil causes a contracture

Fully relaxed muscles were incubated in 2 ml oxygenated Ringer's buffer containing verapamil at several concentrations for one hour. Figure 1 shows percent increases in tension generated in sartorius, semitendinosus and semimembranosus muscles. Data shown represent at least 3 measurements of 3 muscle pairs at each concentration.

Extracellular Ca^{+2} not required for contracture

Muscles were rinsed in 10 mM EDTA (ethylene diamine [N,N,N',N'-tetraacetic acid]) followed by a rinse in calcium and magnesium free Ringer's buffer to remove any EDTA or loosely bound Ca^{+2} . Relaxed muscles were incubated with calcium and magnesium free Ringer's buffer containing various concentrations of verapamil for one hour. The ratio of the tension enhanced by verapamil in calcium free media to that tension caused by verapamil in normal Ringer's is shown in Figure 2.

Effect of dantrolene on the contracture caused by verapamil

Muscles were incubated in 60 μM dantrolene, a blocker of SR Ca^{+2} release (Desmedt and Hainaut, 1977), in Ringer's buffer for 30 minutes. At that time several concentrations of verapamil were added to the tubes and the samples were incubated for an additional hour before measuring muscle tension. Results for untreated controls, verapamil treated and dantrolene and verapamil treated muscles are shown in Figure 3.

Figure 1

A plot of muscle tension in grams versus the concentration of verapamil in mM for three types of muscle is shown. Errors in tension measurement is $\leq 3\%$

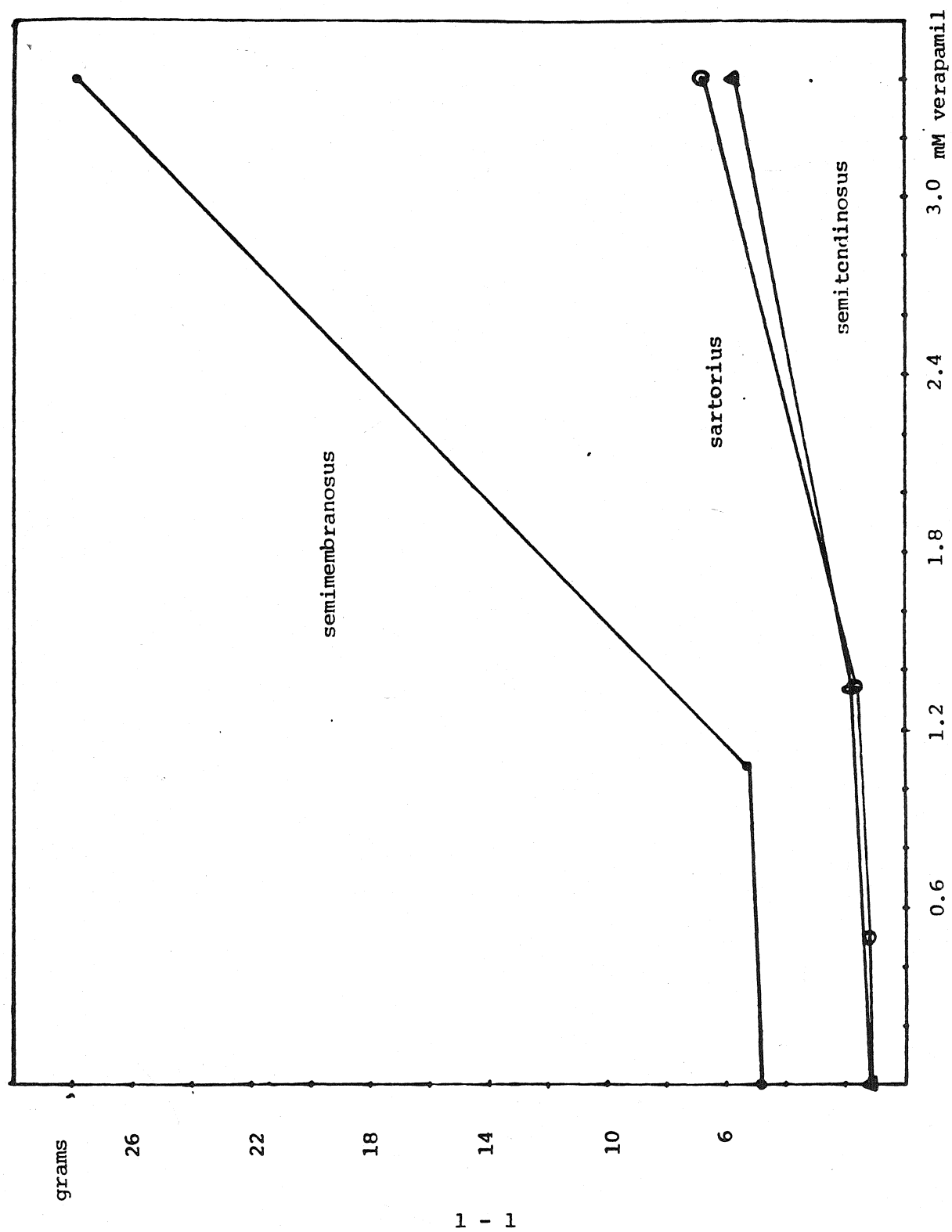


Figure 2

Muscles are rinsed in 10 mM EDTA and then exposed to verapamil in Ca^{+2} free buffer. A ratio of the contracture in the absence of Ca^{+2} to that observed in normal Ca^{+2} buffer is shown in per cent versus the concentration of verapamil in the incubation buffer. Error bars are plotted with each point.

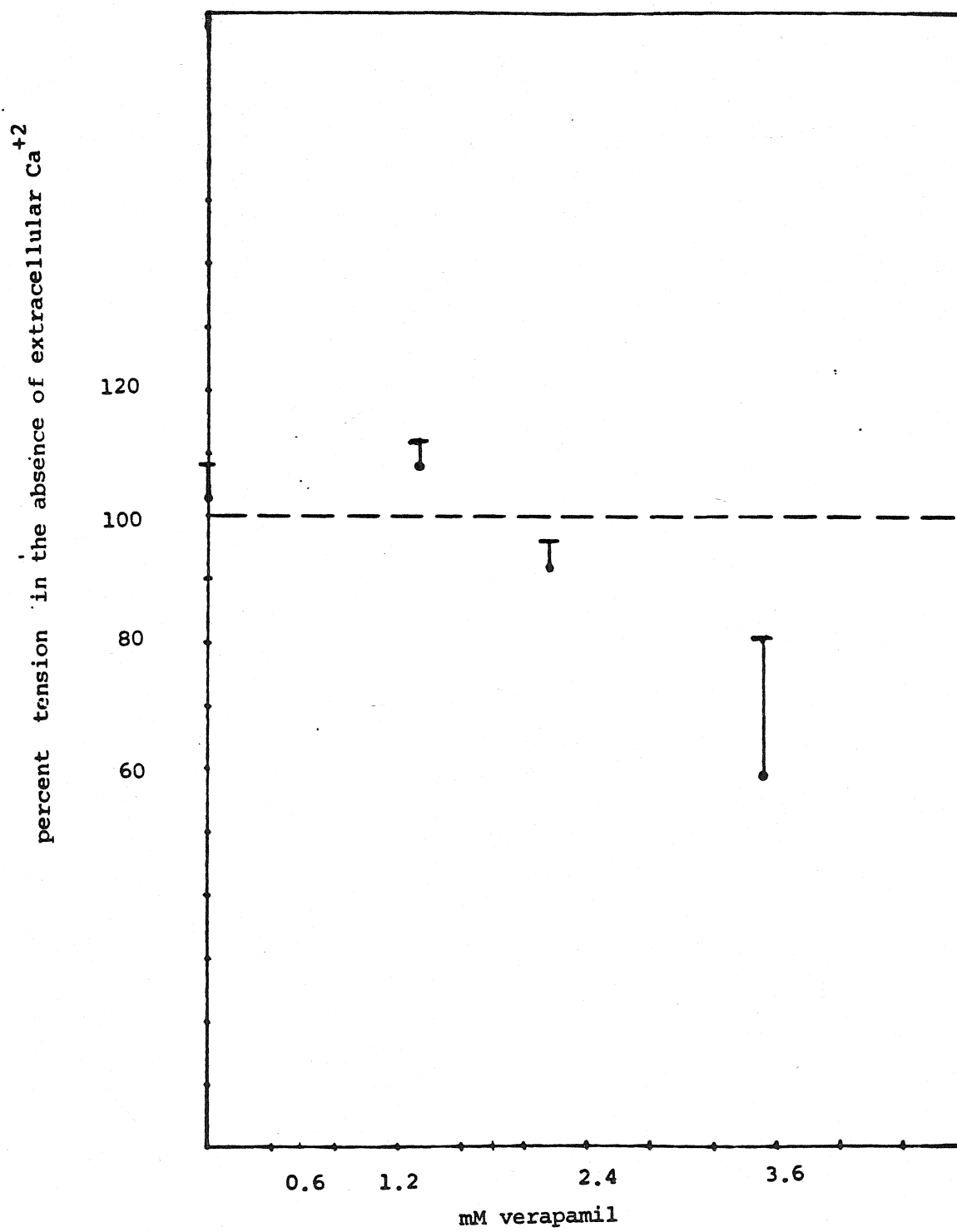
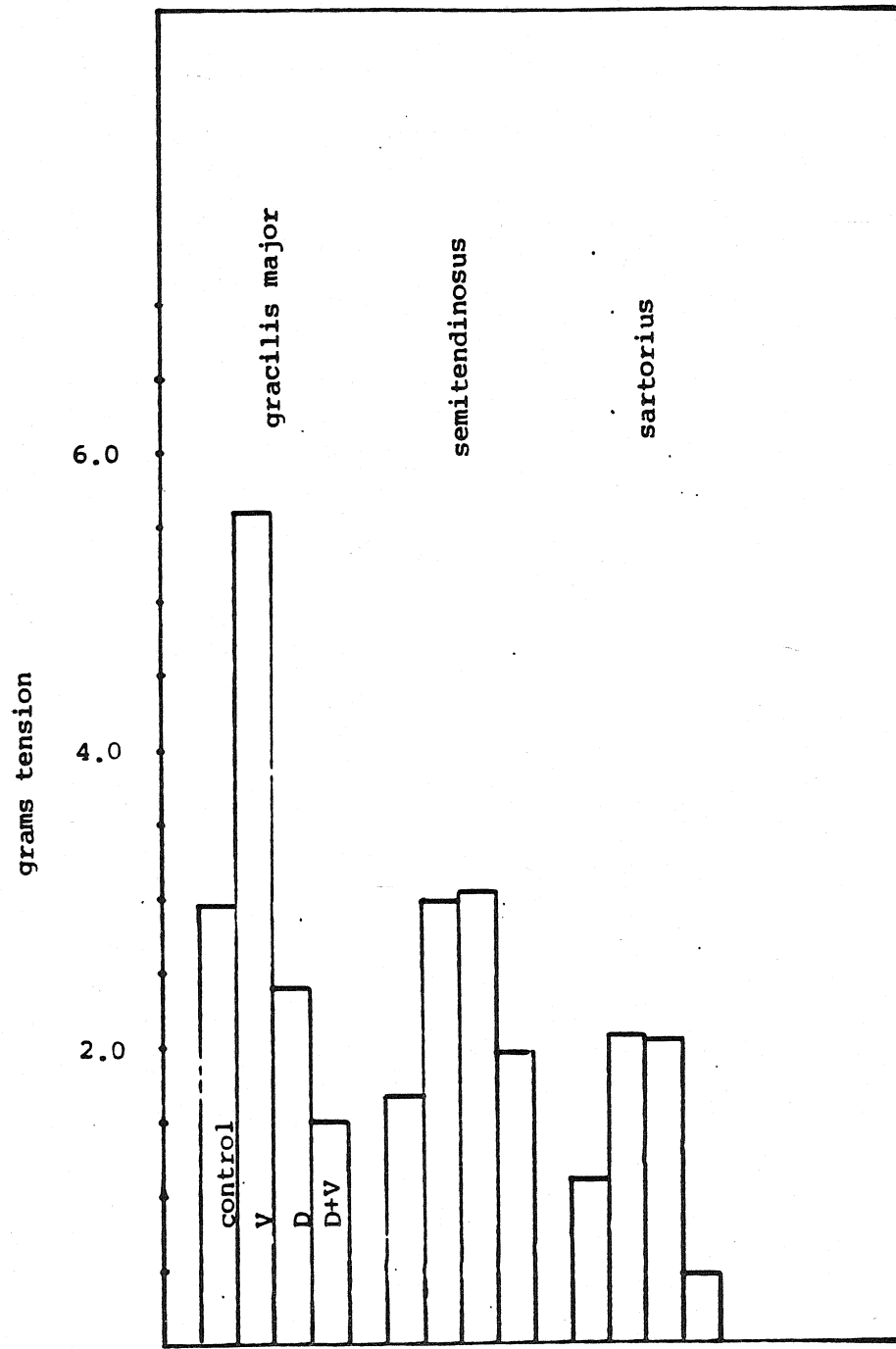


Figure 3

A bar graph showing the tension generated in the presence or absence of dantrolene (60 μ M) on three different types of muscle each at a different level of verapamil. In each set of four experiments are revealed: control tension, tension with verapamil alone, tension with dantrolene alone and tension in the presence of dantrolene and verapamil. The gracilis major (1.1 mM verapamil), semitendinosus (2.5 mM verapamil) and sartorius (3.5 mM verapamil) sets are shown at the left, center and right of the figure, respectively. Error in tension measurement is $\leq 3\%$



Effect of verapamil on muscles treated with hyperosmotic glycerol

Muscles were incubated in glycerol-Ringer's (400 mM glycerol in Ringer's buffer) for 30 minutes. At that time the muscles were rinsed with Ringer's buffer and incubated with verapamil in Ringer's buffer for one hour before measuring tension at rest length. Glycerol treatment resulted in a 70% inhibition of the verapamil induced contracture at 1.2 mM verapamil and a 18% inhibition of the contracture at 2.4 mM verapamil.

Intracellular recording from muscle treated with verapamil

The resting potential of muscle (-65 to -70 mV) was not altered by treatment with up to 3.5 mM verapamil for up to 1.5 hours.

Verapamil does not facilitate the transmembrane flux of Ca^{+2} or Rb^{+} through artificial lipid vesicles

The incorporation of $^{45}\text{Ca}^{+2}$ into vesicles containing 10 mM EGTA in PBS when in the presence of 1 mM or 4 mM verapamil was not statistically different from the incorporation when the vesicles were in PBS alone. In vesicles containing only PBS, Rb^{+} incorporation was not altered by verapamil at the same concentration used to test Ca^{+2} flux.

Effect of verapamil on Rb^{+} efflux in muscle

Figure 4 shows initial rate of $^{86}\text{Rb}^{+}$ efflux relative to total $^{86}\text{Rb}^{+}$ loaded for a number of concentrations of verapamil in the presence or absence of dantrolene (60 μM). At doses below 0.6 mM, a reduction of Rb^{+} efflux is observed, but as the drug concentration is increased, efflux increases to a level about

the same as seen in the absence of verapamil. The increase in efflux of Rb^+ caused by verapamil is blocked by the presence of dantrolene.

Uptake of $^{45}\text{Ca}^{+2}$ into muscle bound stores is enhanced by verapamil at high concentrations

Figure 5 presents the rate of Ca^{+2} uptake into bound stores as a function of concentration of verapamil.

Figure 4

Relative efflux of $^{86}\text{Rb}^+$, the ratio of cpm $^{86}\text{Rb}^+$ released in 5 minutes to the total cpm loaded, versus verapamil concentration is shown. (Solid line-no dantrolene; dashed line- $60\mu\text{M}$ dantrolene) Error bars are plotted on the figure.

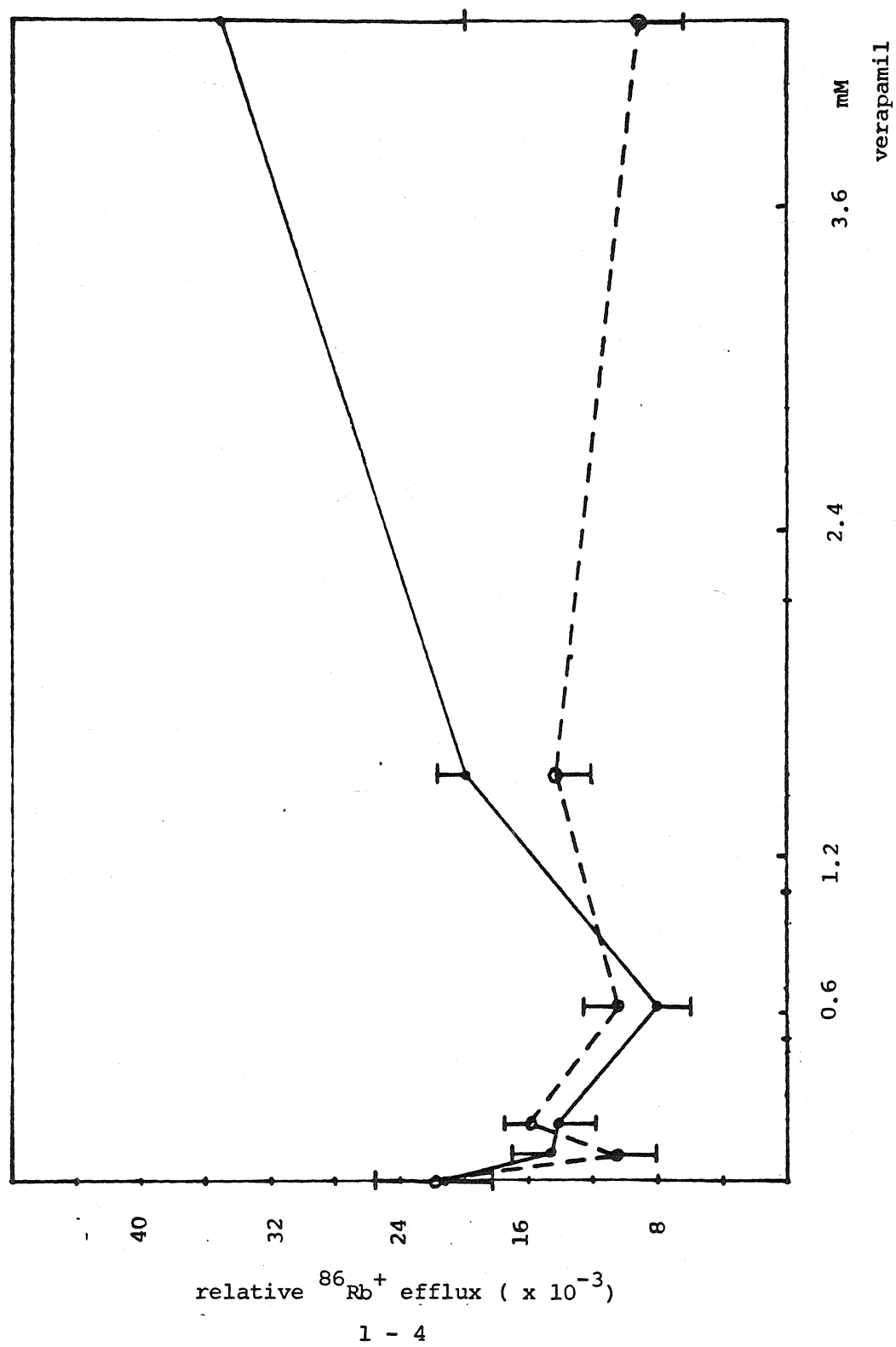
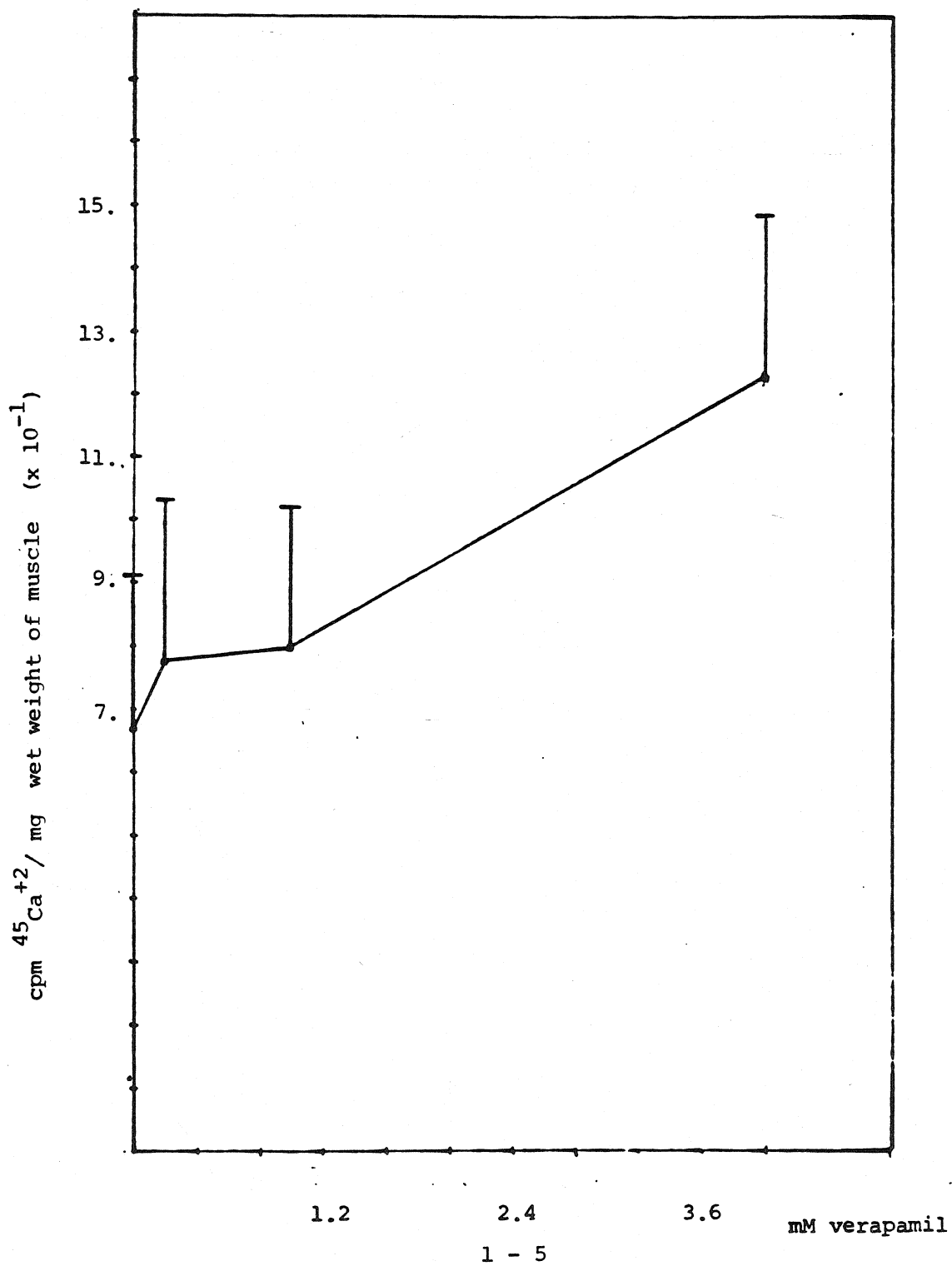


Figure 5

The cpm $^{45}\text{Ca}^{+2}$ taken into bound stores in 5 minutes per mg wet weight of muscle are plotted versus the verapamil concentration. Error bars are plotted with each point.



Discussion

In skeletal muscle, we find verapamil has two effects upon Ca^{+2} metabolism. Verapamil appears to act as a Ca^{+2} antagonist between 0 and 0.6 mM and at concentrations between 0.6 and 4 mM, it can mobilize Ca^{+2} from the SR. We believe that these two effects are a result of the interaction of verapamil with two independent sites on the cell. To activate the release of Ca^{+2} from the SR, the drug must either act on the SR directly or bind to some structure in the t-tubule. The Ca^{+2} -antagonistic effects appear to be mediated generally at the cell surface.

The two effects of verapamil are best visualized in muscle by the Rb^{+} efflux experiments. $^{86}\text{Rb}^{+}$, which behaves as K^{+} in biological systems, is used to monitor the presence of Ca^{+2} dependent K^{+} conductances (Gardos, 1958; Putney, 1979) and alterations in $[\text{Ca}^{+2}]$. While there has been no previous report of such a Ca^{+2} conductance in skeletal muscle, our work with verapamil suggests the existence of one. At low concentrations of verapamil, $^{86}\text{Rb}^{+}$ efflux is reduced. We believe that at these concentrations, Ca^{+2} antagonistic activity of verapamil is evident. The concentration of Ca^{+2} is reduced at the inside of the membrane and so the Rb^{+} efflux is reduced. We are unable to determine whether verapamil acts to block entry of Ca^{+2} as proposed by Fleckenstein and others (Fleckenstein, 1974; Malaisse, et al, 1976; Jetley and Weston, 1976) or whether verapamil modulates some intracellular pool of Ca^{+2} in a way that would reduce $[\text{Ca}^{+2}]$.

at the membrane such as suggested by (Matthews, 1975; Cronin, 1982; Church and Zsoter, 1980). As the concentration of verapamil increases, a second activity becomes apparent. Rb^+ efflux increases and this increase can be blocked by treatment with the drug, dantrolene, which has been shown to block the release of Ca^{+2} from the SR (Desmedt and Hainaut, 1977). Also it could be shown that verapamil did not act directly on the membrane to facilitate the release of Rb^+ , since it was found that the drug did not cause transmembrane flux of $^{86}\text{Rb}^+$ into artificial lipid vesicles. Another verification of the action of verapamil on the SR is seen in that verapamil caused a contracture in muscle that could be inhibited by dantrolene.

Since it was observed that verapamil did enhance the influx of Ca^{+2} into bound stores, some attention must be given to what contribution to the increase in intracellular $[\text{Ca}^{+2}]$ caused by verapamil this Ca^{+2} might play. The amount of Ca^{+2} that enters the cell must however be small compared to the amount arising from the SR since the contracture is inhibited by dantrolene.

We have several pieces of evidence that verapamil acts at a second, independent site to activate the SR. The participation of voltage sensitive Ca^{+2} or Rb^+ (K^+) channels or any voltage sensitive process that allows Ca^{+2} influx or activates the release of Ca^{+2} from the SR can be neglected since treatment of muscle with the drug over the entire dose range (0.1 - 4 mM) does not

alter the cell potential. Additionally, when the muscles were subjected to hyperosmotic shock to disrupt the t-tubule system, the verapamil contracture was inhibited to some extent. We are unsure whether the hyperosmotic shock prevents access of the drug to receptors in the t-tubule or access to the SR membrane itself. The resolution of this question could be valuable to understanding the E-C coupling process. Frank (1979) proposed that Ca^{+2} associated with the t-tubule is released when the action potential arrives at the t-tubule. This Ca^{+2} can then interact with the SR to release a large amount of Ca^{+2} into the cytoplasm. Because the amount associated with the membrane is too small to cause a contraction alone, it is called "trigger" Ca^{+2} . If verapamil also mobilizes trigger Ca^{+2} , then it would be particularly interesting to identify the verapamil receptor. Verapamil, however, may act directly on the SR and bypass the trigger mechanism. In this case, verapamil may be useful to determine how the trigger Ca^{+2} can effect the release of SR Ca^{+2} . Work by Shoshan, etal, (1981) suggests that this activation requires a change in the pH gradient at the SR membrane. To determine the effect of verapamil, if any, on the SR, the drug could be applied directly to SR vesicles and Ca^{+2} release could be measured.

A similarity between E-C coupling and stimulus-secretion coupling is noted as verapamil affects mast cells, the cells that respond to an IgE-antigen complex by secreting histamine, much

like muscle. Histamine release and $^{86}\text{Rb}^+$ efflux show the same biphasic response to verapamil at various concentrations (Herndier, 1981; B. Herndier and J. Richards, to be published).

There may be common receptors on mast cells and muscles or similar patterns of regulation of intracellular $[\text{Ca}^{+2}]$ mediated by verapamil.

References

- Bianchi, C and Shanes, A (1959) J Gen Physiol, 42, 803
- Bihler, I (1972) in The Role of Membranes in Metabolic Regulation
eds. M. Hamman and R. Hanson, Academic Press, New York,
- Caputo, C (1978) Ann Rev Biophys Bioeng, 7, 63
- Church, J and Zsoter, T (1980) Can J Physiol Pharmacol, 58, 254
- Cronin, M (1982) Life Sci, 30, 1385
- Desmedt, J and Hainaut, K (1977) J Physiol, 265, 565
- Ebashi, S (1961) Prog Theoret Phys Suppl, 17, 35
- Ebashi, S and Lipmann, F (1962) J Cell Biol, 14, 389
- Fleckenstein, A (1974) Adv Cardiol, 12, 183
- Frank, G (1979) Proc West Pharmacol Soc, 22, 309
- Gardos, G (1958) Biochem Biophys Acta, 30, 653
- Hansford, R and Chappell, J (1967) Biochem Biophys Res Commun,
27, 686
- Hasselbach, W and Makinose, M (1961) Biochem Z, 333, 529
- Hasselbach, W (1980) Basic Res Cardiol, 75, 2
- Herndier, B (1981) Ph. D. Thesis, C.I.T.
- Jetley, M and Weston, A (1976) Br J Pharmacol, 58, 287P
- Levinson, S, Curatalo, C, Reed, J and Raftery, M (1979) Anal Biochem, 99, 72

Malaisse, W, Devis, G, Pipeleers, D and Somers, G (1976)

Diabetologica, 12, 77

Matthews, E (1975) in Calcium Transport in Contraction and Secretion, eds. E. Carnfoli, F. Clementi, W. Drabikowski and A. Margreth, North Holland, Amsterdam

Putney, J (1979) Pharm Rev, 30, 209

Rasmussen, H (1981) Calcium and cAMP as Synarchic Messengers, J. Wiley and Sons, New York

Schudt, C, Gaerther, U and Pette, D (1976) Eur J Biochem, 68, 103

Shoshan, V, MacLennan, D, and Wood, D (1981) Proc Nat Acad Sci, 78, 4828

Chapter 2

Control of Ca^{+2}

in muscles

by Compound 48/80

Introduction

Compound 48/80 has been found to regulate Ca^{+2} dependent processes in a number of types of cells. In mast cells, Compound 48/80 causes degranulation which releases the vasoactive amines, histamine and serotonin. A key step in the degranulation process is the fusion of the granules with the cell membrane, which requires an elevation in intracellular $[\text{Ca}^{+2}]$ (Hirata and Axelrod, 1980). Drug treatment of smooth muscle (guinea pig intestinal strips) (Kamikawa and Shimo, 1978) and frog skeletal muscle (Herndier, 1981) generates a contracture. While the source of Ca^{+2} for the physiological mast cell response is still disputed (either intracellular and/or extracellular), it is accepted that normal skeletal muscle activation occurs via the release of Ca^{+2} from an intracellular store, the sarcoplasmic reticulum (SR) (Rasmussen, 1981). The process by which a muscle action potential is converted into the release of Ca^{+2} from the SR is called excitation-contraction (E-C) coupling and is still poorly understood. Work by Herndier (1981) suggests that Compound 48/80 does regulate the SR and can cause an elevation of intracellular $[\text{Ca}^{+2}]$. Compound 48/80 may act on some of the elements of the E-C coupling system and, if so, a greater understanding of the effects of Compound 48/80 on muscles may increase our knowledge of the E-C coupling process.

Methods

Frogs

Animals were obtained from Carolina Biologicals.

Rana pipiens of about three inch length were used in these experiments.

Chemicals

Dantrolene was a gift of Norwich-Eaton Pharmaceuticals of Norwich, NY. Compound 48/80 was purchased from Sigma and neuraminidase was purchased from Calbiochem.

Muscles

Muscles were isolated surgically as was described for the work with verapamil (this thesis). Once the muscles were removed, they could be used to test the response to Compound 48/80 or be given some pretreatment such as digestion with neuraminidase before the experiment.

Neuraminidase treatment

Muscles were placed in 2 ml of Ringer's buffer to which was added 1 IU neuraminidase/ml. The digestion was halted after 30 minutes by removing the muscle from the enzyme solution and washing several times with Ringer's buffer.

Measurement of excitation threshold

Muscles were connected to the Combielectrode

and the contraction threshold was found by adjusting the voltage applied to the extracellular electrode. The voltage setting was then doubled and the ratio of the tension generated to the applied voltage was followed with time. At zero time, a given amount of drug was added to the incubation media.

Measurement of force generated by the muscles

Excised muscles were attached to the Combielectrode and transducer as described previously in this thesis. Drug treated muscles were exposed to various doses of Compound 48/80 for one hour before measuring the force at rest length.

Measurement of Ca^{+2} flux into artificial lipid vesicles

Artificial bilayer vesicles were prepared with L- α - phosphatidyl choline as described earlier in the thesis. Both $^{45}\text{Ca}^{+2}$ and Compound 48/80 were added to the samples at zero time and the uptake was stopped by spinning the mixtures through Sephadex G-50 minicolumns.

Results

Compound 48/80 causes a contracture in skeletal muscle in the presence or absence of extracellular Ca^{+2}

When excised muscles were treated with Compound 48/80 in normal Ringer's buffer or rinsed in 10 mM EDTA and incubated in Ca^{+2} free Ringer's buffer with Compound 48/80, a contracture could be observed. The graph in Figure 1 shows the relative increase in muscle tension in grams for several different muscles and concentrations of drug. Contractile response reached a maximum at 250-500 $\mu\text{g}/\text{ml}$ and remained at a plateau at doses up to 2 mg/ml .

Neuraminidase treatment of muscle prevents the Compound 48/80 induced contracture

Muscles that have been treated with neuraminidase do not undergo a contracture when treated with Compound 48/80. Figure 2 shows the tension in different muscles.

Dantrolene inhibits the Compound 48/80 induced contracture in Ca^{+2} free media

Tension generated in muscles incubated with 50 μM dantrolene before Compound 48/80 treatment was significantly reduced when compared to the tension generated in muscles treated with Compound 48/80 alone. The results of this experiment are shown in Figure 3.

Figure 1. The tension generated in muscles treated with various doses of Compound 48/80 and in the presence or absence of extracellular Ca^{+2} is shown. Error bars are standard deviations.

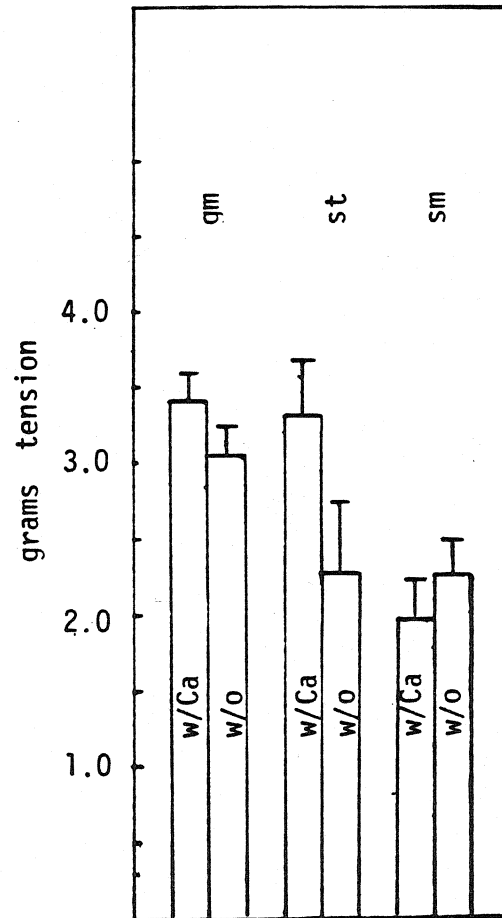
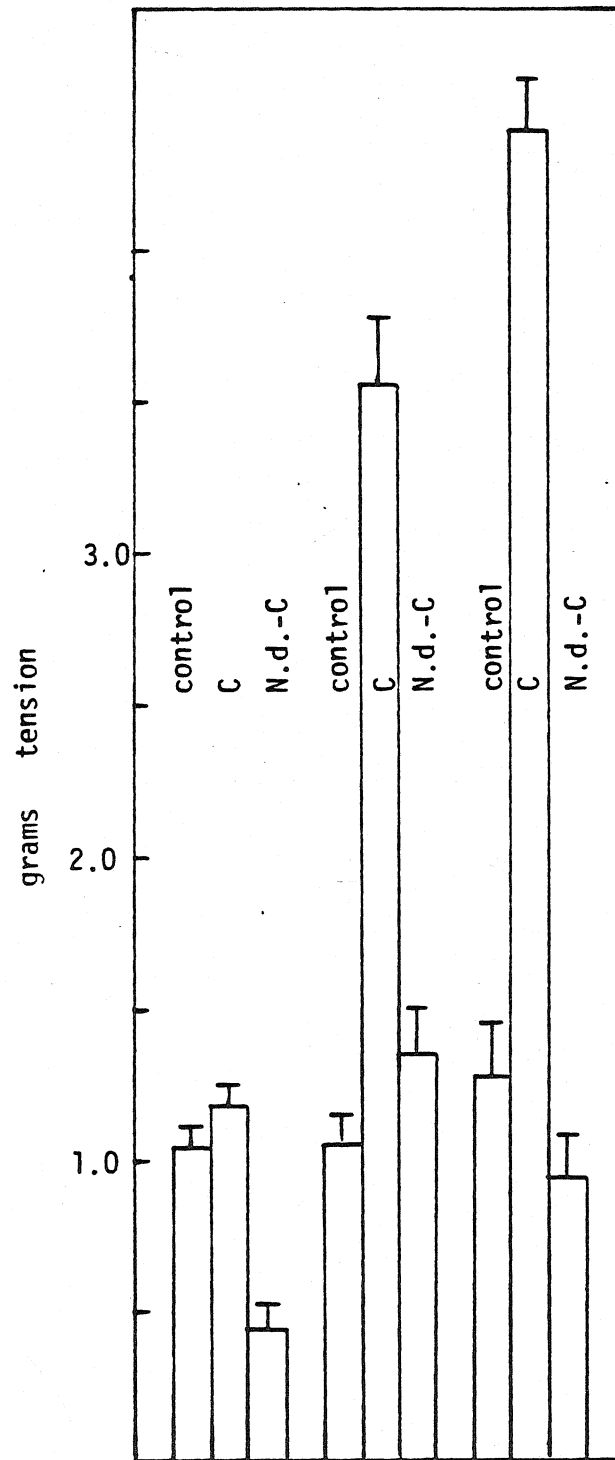


Figure 2. The results of treating a muscle with neuraminidase before exposure to Compound 48/80 are shown in this Figure. For each muscle compared there were three conditions tested: no treatment (control), Compound 48/80 alone (C) and a neuraminidase digestion followed by Compound 48/80 exposure (N.d.-C).



Contraction threshold is elevated by treatment with Compound 48/80

A record of sensitivity (mg of tension generated per mV of extracellular voltage applied) was kept and marked differences between control and Compound 48/80 treated muscles were observed. Control muscles had a $T_{1/2}$ value (time to reduction of sensitivity by one half) of 75 ± 5 minutes and muscles treated with 400 $\mu\text{g/ml}$ Compound 48/80 had $T_{1/2} = 2.07 \pm 0.015$ minutes. During this time, there was little contracture generated by the drug.

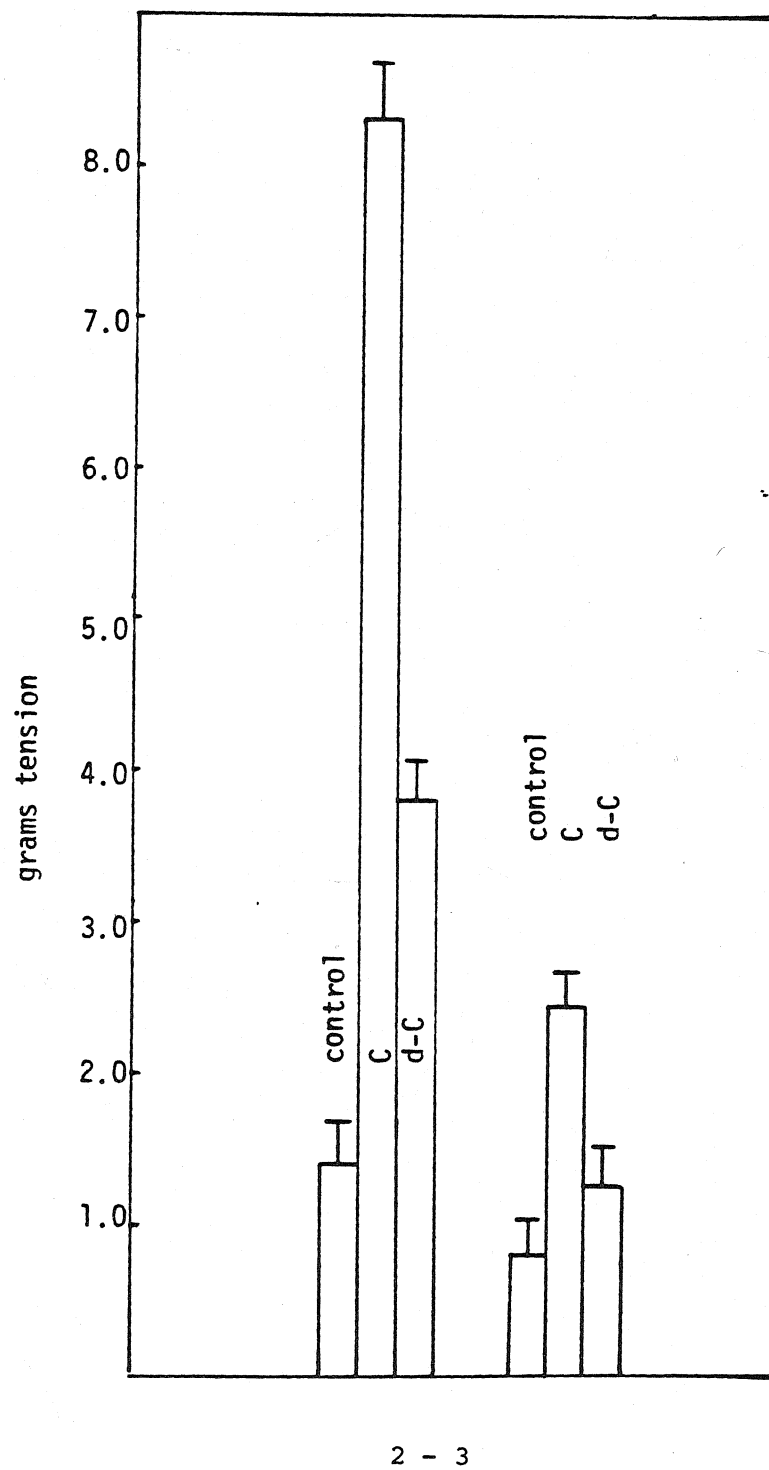
Compound 48/80 interacts with lipid vesicles to enhance transmembrane flux of Ca^{+2}

When vesicles were exposed to 0 and 2 mg/ml Compound 48/80, it was found that the drug caused 2 - 3 fold greater uptake of Ca^{+2} into the vesicles than did the buffer alone.

Compound 48/80 does not affect membrane potential in frog skeletal muscles

Exposure of muscles with up to 2 mg/ml of Compound 48/80 for periods of up to an hour did not alter the membrane potential in skeletal muscle from the value -75 mV.

Figure 3. In this Figure is presented the measurements of effects of dantrolene, a blocker of SR Ca^{+2} release, on tension generated in muscles caused by Compound 48/80. Data are shown for untreated (control), Compound 48/80 only treated (C) and, dantrolene and Compound 48/80 treated (d-C) muscles.

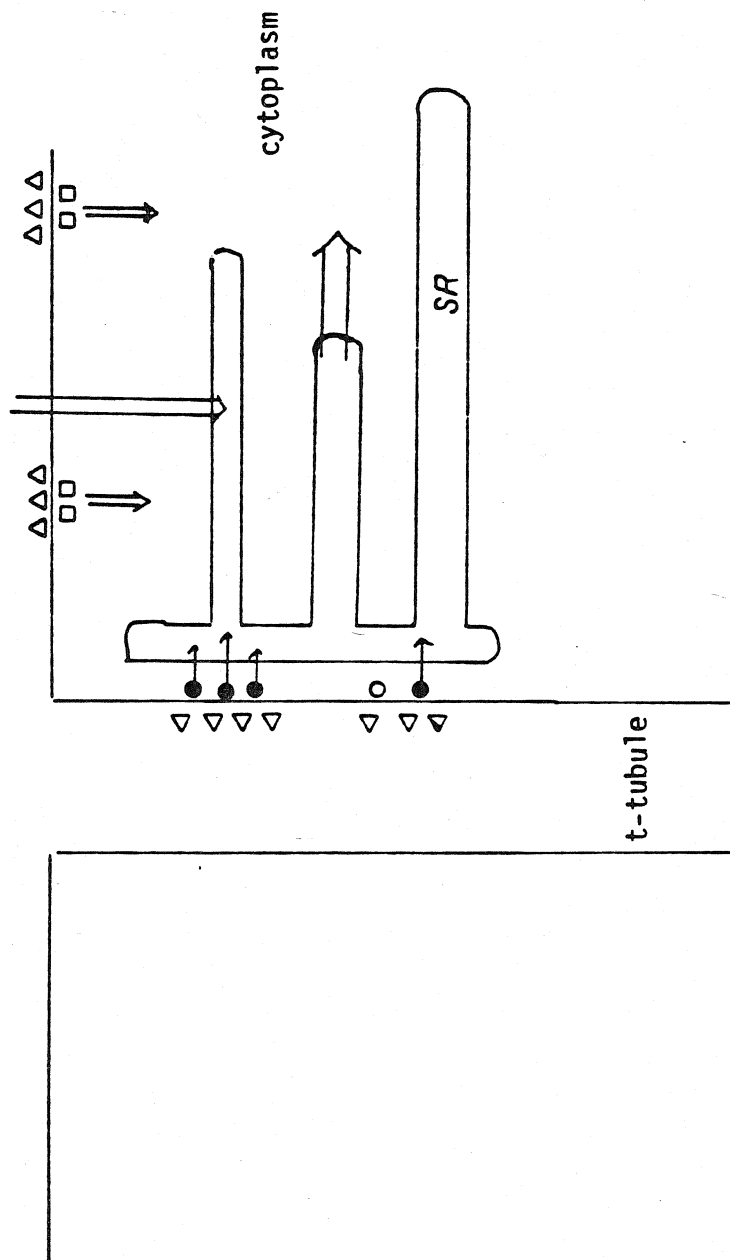


Discussion

The work reported here supports and further details the model of action of Compound 48/80 on muscle presented by Herndier (1981). An illustration of this model is shown in Figure 4. The primary points of the model are that Compound 48/80 acts in two ways upon the muscle - one at the membrane via a neuraminidase sensitive path to elevate intracellular $[Ca^{+2}]$ (and cause contracture) and the other, a neuraminidase resistant pathway that facilitates Ca^{+2} uptake from the extracellular medium into bound stores without elevating intracellular $[Ca^{+2}]$.

The neuraminidase sensitive pathway mobilizes Ca^{+2} from the SR and from a plasma membrane buffer which can be replenished with extracellular Ca^{+2} . That Compound 48/80 can activate the SR is shown by the studies of the effects of dantrolene on tension generated by verapamil in the absence of extracellular Ca^{+2} . Dantrolene, which has been shown to block the release of Ca^{+2} from SR (Desmedt and Hainaut, 1977), inhibits the Compound 48/80 induced contracture by ~70%. The remaining 30% of the Ca^{+2} must come from some other intracellular source. The plasma membrane and mitochondria are both considered elements of the cytoplasmic Ca^{+2} buffer system, but only the plasma membrane has been shown to release Ca^{+2} into the cytoplasm of muscle (Rasmussen, 1981). When Ca^{+2} is present in the extracellular medium, Compound 48/80 not only releases Ca^{+2} from the SR and plasma membrane, but Ca^{+2} outside the cell can enter the membrane pool. This Ca^{+2} from the outside of the cell is not essential for generating the

Figure 4. This Figure presents a model of the muscle consistent with our observations. Sialoglycoproteins are shown as triangles, solid circles represent trigger Ca^{+2} , squares are general membrane-bound Ca^{+2} . Arrows show Ca^{+2} flux in the presence of Compound 48/80 and thickness of the arrow represents a relative magnitude of the flux.



contracture as observed in Ca^{+2} free media with Compound 48/80 alone, but when the muscles are treated with dantrolene in normal Ca^{+2} buffer, a normal contracture is observed (data not shown). These results suggest that the neuraminidase sensitive pathway causes the release of Ca^{+2} from SR and the plasma membrane pool. Thus, the SR and the plasma membrane, when extracellular Ca^{+2} is present, can each raise the cytoplasmic $[\text{Ca}^{+2}]$ to levels that saturate the contractile response (2×10^{-6} M).

Compound 48/80 also acts via a neuraminidase-insensitive path to increase Ca^{+2} influx into bound stores (presumably the SR) without increasing intracellular $[\text{Ca}^{+2}]$ nor leading to a contracture (Herndier, 1981)¹ Herndier, (1981) argued that the Ca^{+2} entering the cell must be rapidly sequestered by the SR and this is consistent with the observations of Compound 48/80 induced tension in neuraminidase treated muscles.

While Compound 48/80 was found to facilitate Ca^{+2} into artificial lipid vesicles, there was little sign that any Ca^{+2} entering by pathways other than through the neuraminidase-sensitive path contributes to the Compound 48/80 induced elevation in intracellular $[\text{Ca}^{+2}]$. This can be seen in that the contracture is abolished by neuraminidase treatment.

A major gap in the understanding of muscle physiology is how the muscle converts an electrical signal at the membrane into the signal that causes the SR to release Ca^{+2} (E-C coupling).

Since sialoglycoproteins do mediate the Compound 48/80 release of SR Ca^{+2} , it would be important to determine the location of these molecules on the surface of the muscle. A tentative effort was made by subjecting the muscles to hyperosmotic shock which causes the t-tubule membrane to be no longer exposed to the surface (Howell and Jenden, 1967). Compound 48/80 induced tension in these muscles were slightly reduced when compared to the tension generated in muscles that were not subjected to the shock. This means that sialoglycoproteins are accessible to the solution and not exclusively located in the t-tubule membrane. Another effect of Compound 48/80 of the muscle may be important to understanding the E-C coupling process. When muscles are treated with Compound 48/80, there is a marked change in contraction threshold. It was previously observed that neuraminidase treatment of muscles elevates contraction threshold (Dörrscheidt-Käfer, 1977). It was suggested that normal activity required an interaction between Ca^{+2} and the sialoglycoproteins. This was presumed to be Ca^{+2} on the exterior of the cell membrane and the drug could possibly displace these ions from the surface prior to activation of the intracellular stores. However, this special Ca^{+2} could be a "trigger" as described by Frank (1979), whereby the action potential normally mobilizes this pool and this released Ca^{+2} triggers the further release of Ca^{+2} from the SR. Thus, this membrane-bound Ca^{+2} acts as a trigger since it alone is insufficient to cause contracture. The level of intracellular $[\text{Ca}^{+2}]$ is

greatly amplified when this trigger interacts with the SR membrane. Additionally, the sialoglycoproteins would be part of the system that translates the action potential into Ca^{+2} release.

While the regulation of Ca^{+2} in muscle after treatment with Compound 48/80 differs from activation after neural stimulation (e.g. Compound 48/80 facilitates Ca^{+2} entry into the cell (Herndier, 1981)), the studies performed with this drug have value in identifying possible elements of the E-C coupling system such as the t-tubule sialoglycoproteins.

References

- Desmedt, J and Hainaut, K (1977) J Physiol., 265, 565
- Dörrscheidt-Käfer, M (1977) J Physiol., 273, 52P
- Frank, G (1979) Proc Wgt Pharmacol Soc, 22, 309
- Herndier, B (1981) Ph.D Thesis CIT
- Hirata, F and Axelrod, J (1980) Science, 209, 1082
- Howell, J and Jenden, D (1967) Fed Proc, 26, 553
- Kamikawa, Y and Shimo, Y (1978) Br J Pharmacol., 64, 511
- Levinson, S, Curatalo, E, Reed, J and Raftery, M (1979)
Anal Biochem, 99, 72
- Rasmussen, H (1931) Calcium and cAMP as Synarchic Messengers,
J Wiley and Sons, NY

Chapter 3

The development of
sarcoplasmic reticulum
in muscle cell culture

Introduction

One of the earliest steps in muscle development is the fusion of myoblasts to form myotubes. This change is accompanied by the reduction of enzymes associated with the proliferation of the myoblast (e.g. DNA polymerase (Stockdale and Holtzer, 1961)) and the increase in the proteins of mature muscle (e.g. the enzymes creatinine kinase and glycogen phosphorylase (Coleman and Coleman, 1968; Shainberg, etal, 1971)). In addition, ultrastructural studies of myotubes reveal that contractile filaments of actin, myosin and tropomyosin (Okazaki and Holtzer, 1965; Coleman and Coleman, 1968) and that the SR (Martonosi, etal, 1977) are being organized.

While a temporal sequence of appearance of the functional elements of muscle has been established, an understanding of the causal relationships and identities of initiators and regulators of the developmental process have yet to be determined. Primary cell culture and serially propagated cell lines have been introduced to aid in this endeavor. The rat myoblast line, L8, (Yaffe and Saxel, 1977) will maintain the proliferative, mononuclear phenotype at low cell density; however, at high density, the cell will fuse to form myotubes and, after fusion, a number of muscle specific proteins have been found (Blau and Epstein, 1979). These cells are also receptive to a number of pharmacological stimuli which can alter developmental progress (Blau and Epstein, 1979) or to compounds which can change the intracellular content

of possible regulatory ions, such as Ca^{+2} (Herndier, 1981).

It was observed in the latter study that Compound 48/80 caused an increase in Ca^{+2} uptake into bound stores. These cells

may also provide a system to observe the development of the elements of the excitation-contraction (E-C) coupling process.

If so, it is important to verify that the SR does develop normally in these cells. This work reports a comparison

between myoblast and myotube stages of the development in L8 cells and, especially, the development of the Ca^{+2} sequestering activity of the SR.

Methods

Cells

L8 cells were a gift from Dr. H. Blau of Stanford University. They were maintained in Waymouth's medium supplemented with 10% fetal bovine serum. Cells were passaged 1:10 or 1:20 and media was changed every five days. A myoblast sample contained greater than 99% myoblasts and a myotube sample contained greater than 98% myotubes as determined by cell counts in at least three 100x fields.

Assay of $^{45}\text{Ca}^{+2}$ uptake into bound stores

The media was aspirated and the cells were washed twice with physiological saline. 2 ml of Ringer's buffer (NaCl 6.78 g/l, KCl 0.18 g/l, MgCl_2 0.4 g/l, tris (hydroxymethyl) aminomethane 1.21 g/l, glucose 1.8 g/l and CaCl_2 0.26 g/l: titrated to pH 7.2 with HCl) was added to each plate. At zero time 0.5 $\mu\text{Ci/ml}$ $^{45}\text{Ca}^{+2}$ and various doses of compound 48/80 were added. After 5 minutes, the buffer was aspirated and the cells were allowed to equilibrate with 2 ml Ringer's buffer 4 times each for 30 minutes. The cells were then scraped off the plate, digested in 0.1N NaOH and aliquots were either counted or assayed for protein by the Lowry (1951) method.

Results

Calcium uptake into bound stores

Compound 48/80 causes an increase in Ca^{+2} uptake into both myoblasts and myotubes. Figures 1a and 1b present values of Ca^{+2} uptake as a function of concentration of Compound 48/80 for myoblasts and myotubes, respectively. Myotubes show ~10-fold greater uptake than myoblasts at all doses of Compound 48/80.

Figure 1a: The results of Ca^{+2} uptake experiments in the presence or absence of Compound 48/80 with L8 myoblasts are shown in this figure. Plotted against the vertical axis are rates of uptake and across the horizontal axis are the concentrations of Compound 48/80 present during the labelling. Error bars show + standard deviation.

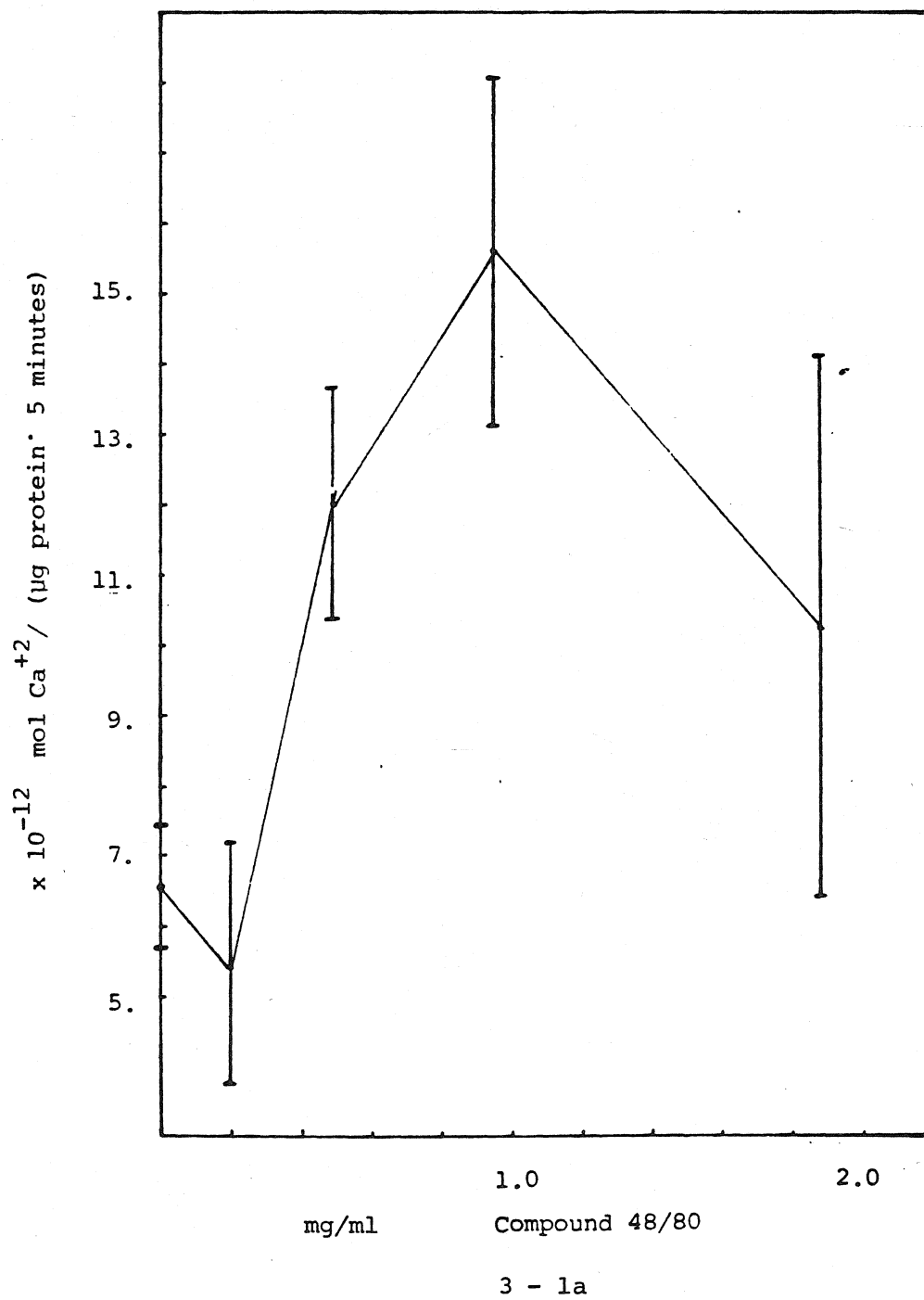
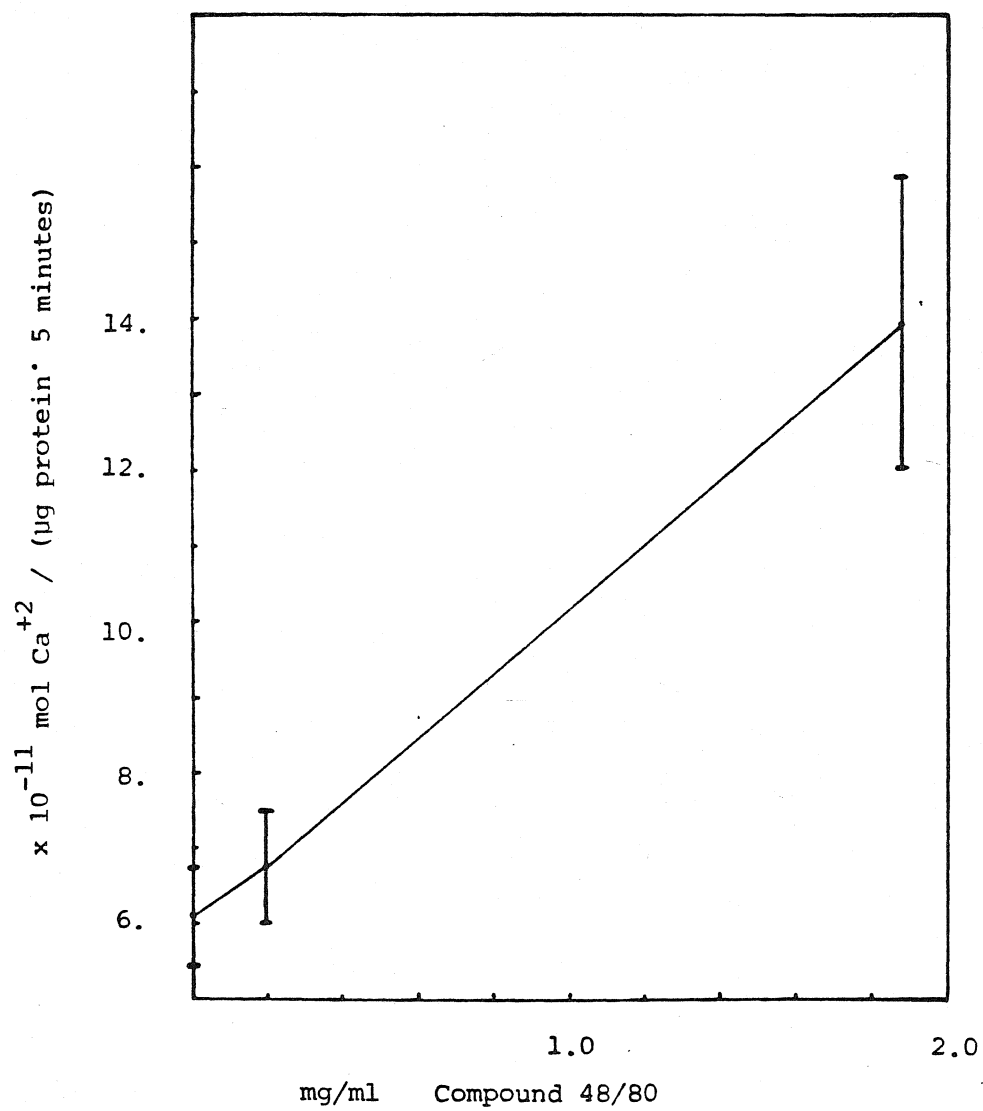


Figure 1b: Rates of Ca^{+2} uptake versus concentration of Compound 48/80 present during uptake are plotted in this figure for L8 myotubes. Error bars show + standard deviation.



3 - 1b

Discussion

Our studies of Ca^{+2} uptake in L8 cells reveal that a Ca^{+2} sequestering activity does appear after fusion of blast-like cells as has been observed in vivo (Martonosi, etal, 1977) and suggest that the SR develops in L8 cells

L8 myotube-like cells show about ten-fold greater uptake of Ca^{+2} than the myoblast-like cells in the presence or absence of Compound 48/80. The difference of uptake in the absence of Compound 48/80 reveals that the difference in the behavior of the two cell types is not just a result of an altered response to the drug. Instead, the increase in Ca^{+2} uptake must be correlated with a developmental change in the cells. Martonosi and others (Martonosi, etal, 1977; Michalak and MacLennan, 1980) have determined the sequence of the development of a number of the proteins of the SR, especially Ca^{+2} -ATPases and calsequestrin, in embryonic tissue or primary cultures of embryonic muscle. In both systems, it was observed that fusion preceded the appearance of the SR membrane and the proteins necessary for the uptake of Ca^{+2} . We argue that a similar developmental pattern occurs in L8 cells; the Ca^{+2} sequestering activity of the SR develops after fusion.

An additional test of the functional integrity of the SR would be to treat the cells with the drug, caffeine. Unlike Compound 48/80, which causes activation of SR and increases Ca^{+2} flux into muscles, caffeine acts specifically to release Ca^{+2} .

from the SR. Any rise in intracellular $[Ca^{+2}]$ would then be a result of the activation of the SR. This cell system could then prove useful in probing the development of muscle, either by isolating mutants or by varying the environment of the cells, e.g. the amount of Ca^{+2} , which has been proposed as a regulator by Martonosi, etal, (1977).

References

- Blau, H and Epstein, C (1979) Cell, 17, 95
- Coleman, J and Coleman, A (1968) J Cell Physiol, 72, Suppl 1, 19
- Herndier, B (1981) Ph. D. Thesis, C.I.T.
- Lowry, O, Rosebrough, N, Farr, A and Randall, R (1951)
J Biol Chem, 193, 265
- Martonosi, A, Roufa, D, Boland, R, Reyes, E and Tillack, T (1977)
J Biol Chem, 252, 318
- Michalak, M and MacLennan, D (1980) J Biol Chem, , 1327
- Okazaki, D and Holtzer, H (1965) J Histochem Cytochem, 13, 726
- Shainberg, A, Yagil, G and Yaffe, D (1971) Dev Biol, 25, 1
- Stockdale, F and Holtzer, H (1961) Exp Cell Res, 24, 508
- Yaffe, D and Saxel, O (1977) Differentiation, 7, 159

Chapter 4

Studies of the mechanism of

nafenopin

Introduction

The cells in the adult liver rarely undergo mitosis and the entire organ maintains a constant mass relative to body weight. (Bucher and Malt, 1971). However, there are a number of stimuli that can increase protein synthesis in the liver such that the relative mass is elevated and such stimuli can also initiate cell division. Sometimes the growth responses are limited such that the liver returns to normal relative mass in time (Bucher and Malt, 1971). Studies of these processes can offer many insights into the regulation of growth in cells.

A comparison of the responses in liver to a number of chemically or surgically induced growth states reveals that each stimulus in some way reduces the functional mass of the liver. Liver growth, therefore, ensues to restore effective mass by an increase in protein synthesis and/or cell division. For example, partial hepatectomy or hepatotoxic agents physically remove or destroy portions of the liver and this can lead to a restoration of mass achieved by increased protein content per cell and by the formation of new cells (Bucher and Malt, 1971). Another group of stimuli appear to interfere with the normal function of liver by competing with other substrates for the mixed function oxidase system. This usually leads to increased protein synthesis, especially of the oxidase system, but rarely do these compounds

initiate cell division (Schulte-Hermann, 1974). Other inducers inhibit other enzyme systems; these can lead to both hypertrophy and hyperplasia (Schulte-Hermann, 1974). In each of these situations, the liver reacts to some metabolic overload and growth is a compensatory response.

One of the compounds that induces hypertrophy and hyperplasia without any cytotoxic effects is nafenopin (2-methyl, 2-(4-(1,2,3,4-tetrahydro-1-naphthyl)phenoxy)propanoic acid). It is a member of a large number of phenoxyacetic acids that are powerful hypolipidemics (Benzce, 1973). After a single feeding of 500 mg nafenopin/kg (body weight), growth is induced in rat liver. However, this growth is reversible since the normal relative mass is restored in 7 days after the feeding (Levine, etal, 1977). Other studies of the effects of nafenopin on liver show that the drug inhibits lipid synthesis from acetyl CoA (Maragoudakis, 1969), causes the proliferation of peroxisomes and endoplasmic reticulum (Reddy, etal, 1973), activates a lipid oxidase system (Reddy, etal, 1981) and alters the production of bile and bile salts and the secretion of compounds into the bile (Levine, etal, 1975).

Levine, etal, (1977) have made comparisons of the effects of nafenopin and partial hepatectomy and have found a number of similarities in the biochemical response. Changes in amino acid transport, nucleoside uptake and DNA synthesis followed nearly

identical time courses.

Nafenopin has also been tested on a number of liver cell lines and one lung cell line (Handly, 1977). In each system, it was found that the drug inhibited cell division and DNA synthesis. DNA synthesis was also found to be inhibited in primary hepatocyte culture (T. Valenzuela, private communication).

Thus, there is a striking difference between the effects of nafenopin observed in vivo and in vitro. This difference may be explained by arguments that the cultured cells are really not like the intact liver or that there is some trophic and/or tropic factor present in the animal that is not in the medium.

This work reports further studies of the effects of nafenopin on cells in culture and some comparisons of the disposition of the drug in both liver and cells in culture.

Methods

HTC Cells

These cells were obtained from the Cell Bank of UCSF. They were grown as monolayers in Eagle's Minimal Essential Medium supplemented with 10% fetal bovine serum. Penicillin, 100 U/ml and streptomycin sulfate, 100 mg/ml, were added to control bacterial growth. Cells were passaged approximately every 5-7 days by aspirating the media, washing the cells with Dulbecco's phosphate buffered saline without calcium or magnesium (DPBS, Dulbecco and Vogt, 1954) which was composed of 2.7mM KCl, 1.5mM KH_2PO_4 , 0.136M NaCl and 8.1mM Na_2HPO_4 , and finally treating the cells with 0.125% trypsin in DPBS for two to three minutes or until the cells could be detached from the plate with gentle aspiration with a Pasteur pipet. Cells (trypsinized suspensions) were divided routinely 1:20 into fresh medium.

P815 Cells

P815 cells were grown in suspension in Dulbecco's modified Minimal Essential Medium supplemented with 10% bovine serum and containing 100 U/ml penicillin, 100 mg/ml streptomycin sulfate to control bacterial growth. Cells were subdivided by diluting 1:10 or 1:20 into plates or flasks with fresh media.

Lysobacter enzymogenes

These bacteria and information about culture techniques were kindly provided by R. Kaiser. Cells were grown at 30°C in medium composed of tryptone 2.0g/l, casamino acids 2.0g/l, monosodium glutamate 20.0g/l, NaCl 2.0g/l, $K_2HPO_4 \cdot 3H_2O$ 2.0g/l, $MgSO_4 \cdot 7H_2O$ 1.0g/l, KNO_3 0.50g/l, $FeSO_4$ 1 mg/ml, $ZnSO_4$ 1 mg/ml $MnSO_4$ 1 mg/ml and sucrose 10g/l. The final pH was adjusted to 7.1 - 7.2. Flasks were placed on a rotary table to provide aeration.

E. coli containing pBR322

The strain LS1 was obtained from Dr. A. Riggs at the City of Hope. Cells were grown at 37°C in FB broth (25.0g/l tryptone, 7.50g/l yeast extract, 102mM NaCl and 0.02M tris (aminomethyl) methane-Cl pH 7.5. Tetracycline (20 mg/ml) was added to prevent growth of any bacteria not containing pBR322.

Assay of DNA synthesis

DNA synthesis was monitored by determining the cpm of tritiated thymidine incorporated into 5% trichloroacetic acid precipitable material for 1 hour of labelling. Results were expressed as cpm/ 10^6 cells or cpm/mg cell protein. Tritiated thymidine was added to cells at a final concentration of 1 μ Ci/ml. At the end of one hour, the media was aspirated and the cells washed in DPBS before trypsinization and counting (HTC cells) or P815 cells were counted and

centrifuged. Cells were then washed once with DPBS to remove trypsin and aliquots for Lowry assay were taken. The remainder of the cells were treated with 5% trichloroacetic acid (TCA) at 4°C overnight. The precipitate was counted either by collection on membrane filters (Whatman GF/C) and once dry, immersed in scintillation fluid or by hydrolysis of the precipitate with 1N NaOH at 100°C for 15 minutes followed by cooling, neutralization with 1N HCl and adding to scintillation fluid.

Determination of Thymidine metabolism

HTC cells with or without previous drug treatment were harvested and sonicated in sonication buffer (0.23M sucrose, 5mM KCl in DPBS). The suspension was centrifuged at 105 kg for one hour at 4°C and the supernatant was collected. The activity of phosphorylating enzymes were measured by adding aliquots of the supernatant to tritiated thymidine in reaction buffer (10mM adenosine -5-triphosphate, 12mM 3-phosphoglyceric acid, 10mM MgCl₂ in DPBS). After one hour at 37°C the sample was frozen at -15°C or immediately chromatographed on TLC plates of cellulose/F or PEI/cellulose and developed with n-propanol-3% ammonia (2:1) or 1M LiCl, respectively. Bands or spots were scraped from the plate and added directly to scintillation fluid for counting.

Measurement of protein synthesis

Protein synthesis was determined by measuring the cpm

of tritiated leucine incorporated into TCA precipitable material for varying labelling durations and the values were expressed cpm/ 10^6 cells-hr.

Tritiated leucine was added to cells at a final concentration of 1 μ Ci/ml. At the end of the labelling period, the cells were washed with DPBS, trypsinized, counted and treated with TCA overnight at 4°C. The precipitate was collected on membrane filters (Whatman GF/C) and after drying, was immersed in scintillation fluid for counting.

Determination of total protein (Lowry)

The determination of the amount of protein in samples was done by the method of Lowry, etal (1951).

Assay for a serum factor after Nafenopin treatment that could stimulate growth

Sprague-Dawley rats (300 g) were given 500 mg nafenopin/kg body weight by gavage or a sham feeding. (The nafenopin was dissolved in polyethylene glycol-400 to give a 200 mg/ml solution). After 12 hours, blood was collected. After clotting, the serum was membrane sterilized (Millipore, 0.22 μ m nominal pore size) and frozen for later use. Cultures of HTC cells were allowed to grow to $1-2 \times 10^5$ cells/plate, before changing media to a low serum level-MEM supplemented with 0.5% fetal bovine serum. When cells

reached a stationary growth stage as determined by cell counts, fetal bovine, polyethylene glycol fed or nafenopin fed rat serum were added to the cells at a final concentration of 10%. After 24 hours, DNA synthesis was measured.

Measurement of penicillinase activity

Penicillinase activity was measured essentially as described in Waley (1974) which relies on the difference in UV absorbance, between penicillin-G and penicilloate. Aliquots of E.coli are centrifuged and resuspended in the assay buffer (100mM sodium phosphate pH 7.0) for sonication. The assay was run as follows: 2.5 ml H₂O, 100 μ l of 0.2M sodium phosphate pH 7.0, and 50 μ l of 50mM penicillin-G were mixed in a cuvette and at zero time, 50 μ l of sonicated extract was added to the cuvette. The reaction was monitored at 240nm with the temperature held at 30°C. $\Delta\epsilon/E$ (mM) was taken to be 0.5. A portion of the sonicate was reserved for protein assay and results were presented in mkat/mg cell protein.

Assay for α -Lytic protease

The activity of this enzyme was measured by adding bacterial enzyme extracts to a reaction mixture composed of 10mM tris (aminomethyl) methane-HCl pH 8.0, 0.1 M KCl and 0.50mM N-acetyl-L- alanine-L-proline-L-alanine-p-nitro-anilide. The product, p-nitroaniline, was monitored at

410nm. ($\Delta\epsilon$ (molar)= 8.86×10^3).

Synthesis of [^{14}C] nafenopin

1. Synthesis of 4 phenyl butanoic acid from 1-bromo-3 phenylpropane.

0.24g of magnesium (70-80 mesh) was added to 10 ml of anhydrous ethyl ether in a 50 ml round bottom flask with stirring. 2.0g of 1-bromo-3-phenylpropane was added to 10 ml of anhydrous ethyl ether and admitted dropwise to the magnesium suspension. The flask was then warmed to initiate the formation of the Grignard reagent, but later removed as the reaction was self-sustaining. When the addition was complete, the solution was refluxed for one hour and allowed to cool. The flask was then attached to the special vacuum line connector, cooled to liquid nitrogen temperature and evacuated while kept in liquid nitrogen. 0.5g dry ice was pulverized and placed within the finger of the apparatus while cooled with liquid nitrogen and evacuated as well. The finger and reaction flask were isolated from the vacuum source, the finger allowed to warm and CO_2 was cryo-pumped into the reaction flask. A breakseal ampoule of $^{14}\text{CO}_2$ (100 mCi) was connected and the $^{14}\text{CO}_2$ was transferred to the reaction flask in the same way. The apparatus was then removed from the vacuum line and constrained to prevent the release of CO_2 . After 24 hours, the unit was opened

and 15 ml of 6 N HCl was carefully added to the flask to decompose the remaining Grignard reagent and dissolve and hydrolyze the magnesium salts. The layers were separated (saving the ether layer) and the aqueous layer was further extracted with ether. The ether extracts were combined with the original ether layer and then extracted three times with 15% NaOH, the aqueous phase was acidified with H_2SO_4 and finally extracted three times with ether. The ether was dried with MgSO_4 and removed by rotary evaporator to give the acid (1.3 - 1.5g, 52-54°C m.p., white oily flakes).

2. Synthesis of α -tetralone (1-one-2,3,4-trihydronaphthalene)

8g of P_2O_5 powder was added to 6 ml of concentrated H_3PO_4 with stirring. When the mixture had cooled to 100° - 120°C, 1g of 4-phenylbutanoic acid was added and kept within these temperatures for one hour, during which time the color turned from yellow to reddish brown. 20 ml of water was added and when cool, the mixture extracted three times with ether. The ether extracts were combined, washed with water, 5% NaOH, water, 3% acetic acid, and finally once more with water. The ether was then dried with MgSO_4 and removed by rotary evaporation to yield the ketone (0.9g yellow oil).

3. Synthesis of 1-hydroxy-1,2,3,4-tetrahydronaphthalene

1g of ketone was dissolved in 10 ml of 90% ethanol and 1g of NaBH_4 (8 fold molar excess) was added and stirred for 4 hours at room temperature. 50 ml of 0.1 N NaOH was added to hydrolyze the boroether and the solution was extracted three times with ether. The extracts were combined and washed with saturated NaHCO_3 water, 0.1 N HCl and water before drying with MgSO_4 . The ether was removed to give 1g of the alcohol. (α -tetralol)

4. Synthesis of 4-(1,2,3,4-tetrahydro-1-naphthyl) phenol

2.5g AlCl_3 and 4g phenol were added to 10 ml hexane in a round bottom flask with stirring. 3g of α -tetralol was dissolved in 10 ml hexane and added dropwise. As the reaction progressed, HCl was liberated and a yellow orange color was formed. Stirring was continued overnight when 20 ml 6 N HCl was added and the flask was cooled on ice. The solid was filtered and washed with hexane-6 N HCl (1:1) and then hexane to give the product (yield ~ 70%, m.p. $124^\circ - 126^\circ\text{C}$)

5. Synthesis of 2-methyl-2-(4-(1,2,3,4-tetrahydro-1-naphthyl) phenoxy propanoic acid (nafenopin)

2g of NaOH, 2.24g of the phenol derivative and 50 ml of acetone were mixed in a 250 ml round bottom flask. 1.3g CHCl_3 was dissolved in 10 ml of acetone and added

dropwise to the mixture with stirring. After completion of addition, the mixture was refluxed for 2 hours. The suspension was cooled with ice, filtered and the solid was slurried with 25 ml water and then acidified with 2 ml of concentrated HCl. The slurry was extracted three times with methylene chloride and the combined extracts were washed with water and dried with MgSO_4 . The volume was reduced by two-thirds and an equal volume of "hexanes" was added. The solution was stirred overnight at 4°C and the solid was filtered, washed with hexane and air dried to give nafenopin (m.p. $131^\circ\text{--}134^\circ\text{C}$, 60% yield)

Results

Nafenopin inhibits DNA synthesis and cell division in cultured mammalian cells

Figures 1a and 1b show the effects of nafenopin treatment on DNA synthesis in HTC cells and P815 cells. Above 250 μM , nafenopin causes HTC cells to detach from the substrata and leads to lysis and cell death.

Effect of nafenopin on thymidine phosphorylation

Table I shows the results of treating HTC cells or HTC cell extracts with 182 μM nafenopin. The phosphorylation of thymidine is only inhibited when intact cells were treated with the drug for 48 hours.

Nafenopin inhibits bacterial growth and specific protein synthesis

Figure 2 shows growth curves for Sorangium sp and the specific activities of α -lytic protease are shown in Table II for several doses of nafenopin. The same information for E.coli LS1 is shown in Figures 3a and 3b, respectively.

Determination of the distribution of nafenopin in rats and HTC cells

Table III shows the results of differential centrifugation studies of [^{14}C] nafenopin treated liver and HTC cells that have been sonicated. In addition, the measurement of radioactivity in serum and liver at 16 hours after feeding gave the values of 1 mM and 10 mM, respectively, in these pools. HTC cells exposed to 30 μM nafenopin contained 30 μM nafenopin after 24 hours.

Figures 1a and 1b

The rate of DNA synthesis in HTC cells (Figure 1a) and P815 cells (Figure 1b) are shown for several doses of nafenopin. Measurements were made after 48 hours of drug exposure. Error bars show standard deviations of mean.

$\times 10^3$ cpm / μ g protein \cdot hour

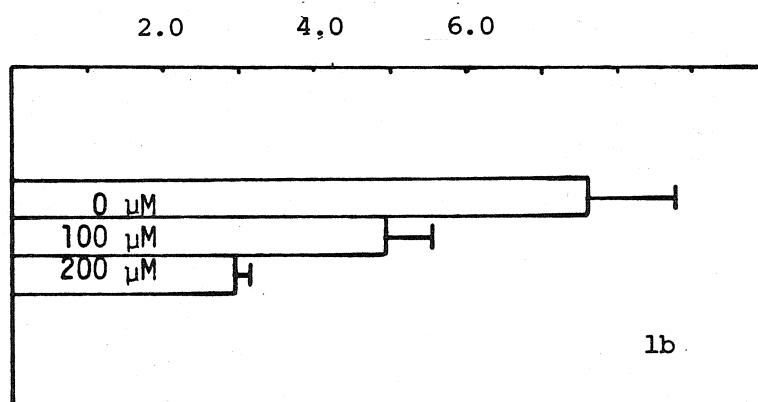
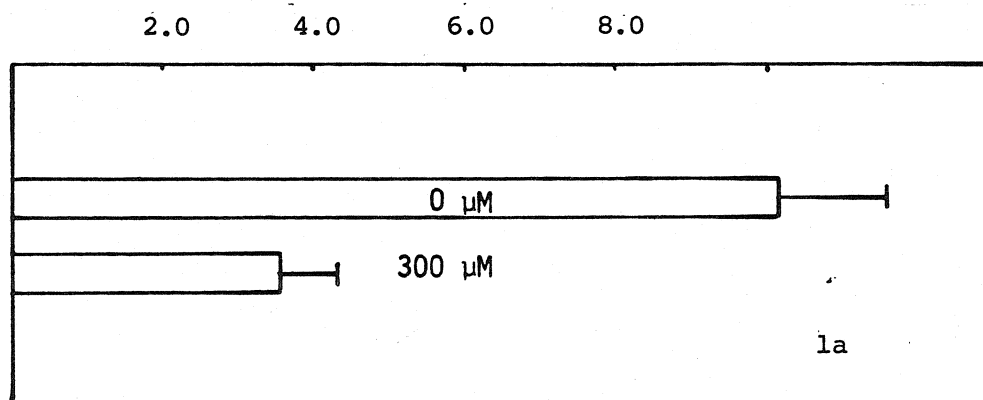


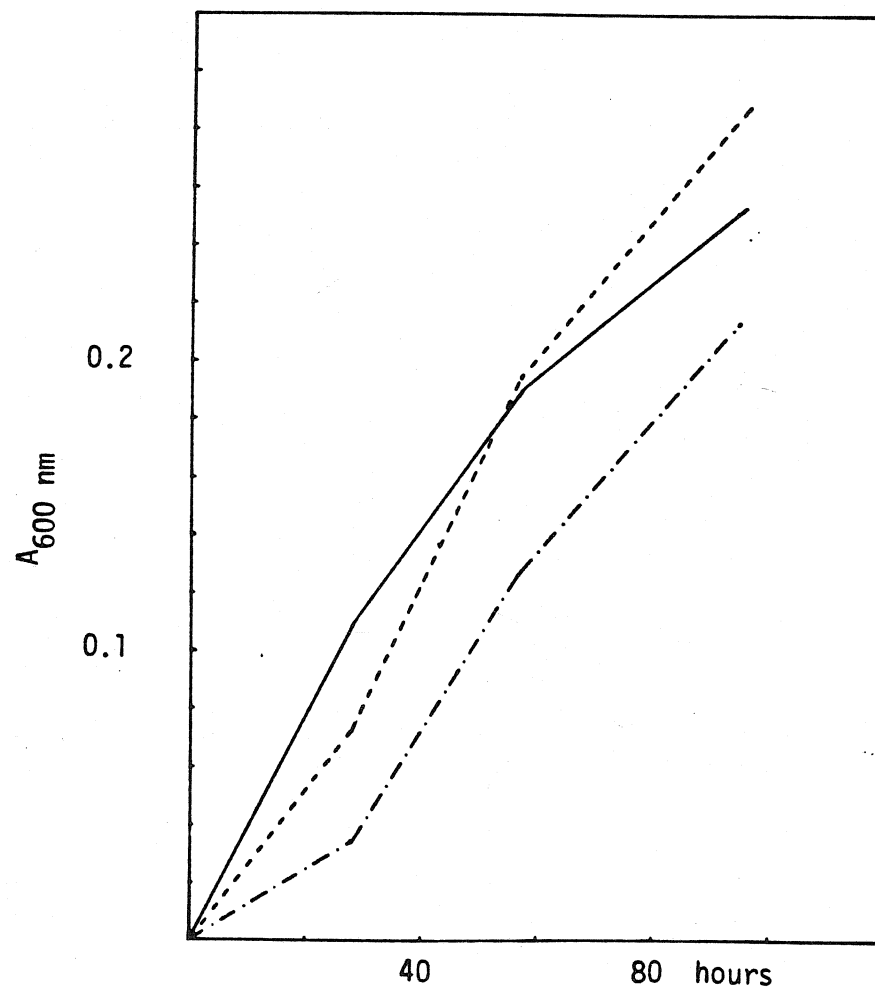
Table I

The fraction of total counts present as thymidine, thymidylate and as summed thymidine di- and triphosphates are shown. The four samples are identified by the presence or absence of 182 μ M nafenopin at different points in the experiment - during cell growth (Time 1) and during the reaction of the cell free extract with labelled thymidine (Time 2). The "Control-Control" sample had no drug present either time, the "Control-Treated" sample had nafenopin present only during Time 2, the "Treated-Control" sample had nafenopin present only during Time 1 and the "Treated-Treated" sample had drug present both times. Errors are estimated to be \pm 7%.

sample	thymidine	thymidylate	di- and tri-phosphorylated thymidine
Control-Control	0.22	0.76	0.02
Control-Treated	0.25	0.73	0.02
Treated-Control	0.98	0.01	0.01
Treated-Treated	0.98	0.01	0.01

Figure 2

This figure presents the growth of Lysobacter enzymogenes as measured by light scattering at 600 nm versus time after inoculation and grown in the presence of no nafenopin (—, solid line), 322 μM nafenopin (---, dashed line) and 484 μM nafenopin (— . —).



Serum from nafenopin fed rats does not induce DNA synthesis in serum starved HTC cells

When nafenopin treated rat serum was added to serum starved HTC cells, there was no stimulation of DNA synthesis when compared to the effects of the serum from rats fed polyethylene glycol alone.

Nafenopin does not inhibit protein synthesis in HTC cells

HTC cells were grown in the absence or presence of 150 μM nafenopin for 48 hours. An assay of protein synthesis revealed values of $1.33 \pm 0.21 \times 10^3$ and $1.33 \pm 0.5 \times 10^3$ cpm [^3H]-leucine incorporated per hour per mg cell protein for the cells exposed to 0 and 150 μM nafenopin, respectively.

Table II

Values of α -lytic protease specific activity (rate/ A_{600})
of unsonicated bacteria relative to untreated bacterial
extracts are shown for two concentrations of drug and at two
times after inoculation.

dose time	42 μ M	177 μ M
24 hrs	0.54	0.19
120 hrs	0.98	0.22

Figure 3a

The growth of E.coli LSl (as measured by light scattering at 550 m) versus time is shown in this figure. Cultures were exposed to 0 μ M nafenopin (——, solid line), 125 μ M nafenopin (---, dashed line) or 1 mM nafenopin (—.—.).

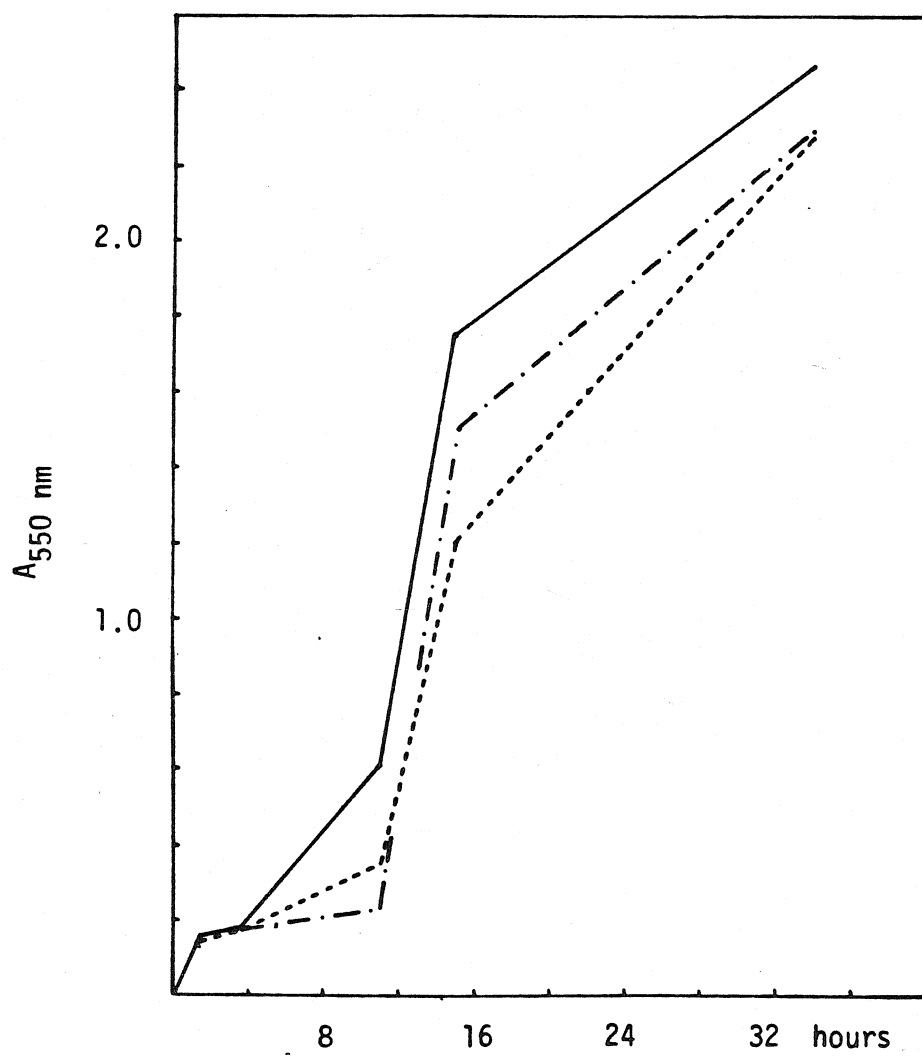
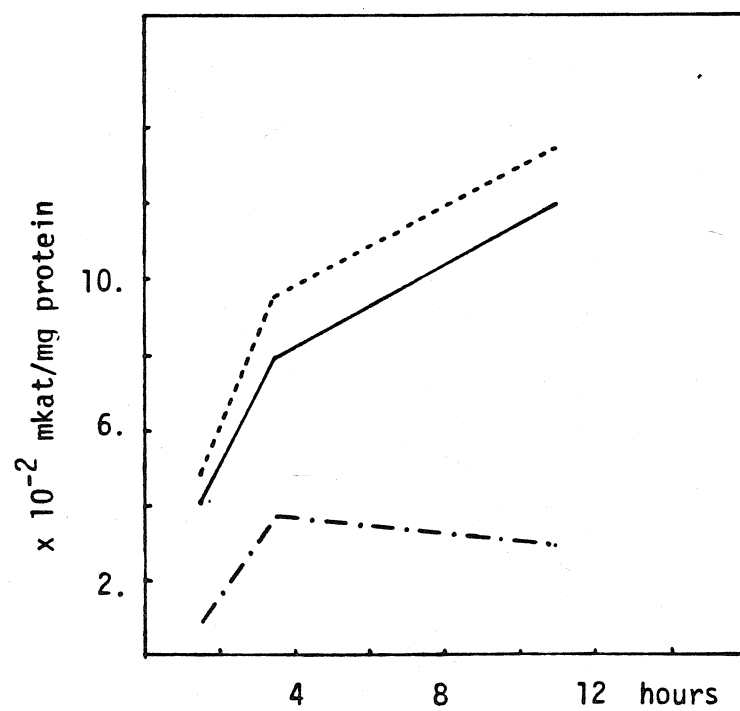


Figure 3b

The specific activities of penicillinase (RTEM) in 10^{-2} mkat/mg protein are shown versus length of treatment with drug control, (——, solid line) 97 μ M nafenopin (----, dashed line) and 1 mM nafenopin (- · -) exposures.



Our evidence shows that nafenopin inhibits growth in a number of cell systems and implies that the cells in the liver that contain the drug after feeding cannot participate in the wave of mitosis. However, the drug was found to have no effect on general protein synthesis, so there should be no effect on the hypertrophic response. This would suggest that there are two compartments (of cells) in the liver, one, the hepatocyte, which actively sequesters and deactivates the drug, and another, possibly a hepatocyte stem cell, which can be recruited to divide to help restore functional liver mass.

Growth (either as cell division or DNA synthesis) was inhibited in all cultured cells tested. Bacteria were, however, able to recover from the inhibition. In addition, it was found that the activities of several enzymes when expressed relative to an A_{600} (light scattering measurement proportional to cell number) or bacterial protein were inhibited by the drug. Thymidine kinase activity was drastically reduced in HTC cells in a roughly dose dependent manner and since the liver is found to have doses of nafenopin several fold higher than that observed to cause the inhibition in vitro, these liver cells would likewise be unable to synthesize DNA. However, DNA synthesis is indeed observed after feeding in the rat so some cells must be free of the inhibitory action of the drug.

Our results show that the average liver cell concentration of nafenopin is 10 times greater than in serum which suggests

Table III

The distribution of nafenopin in rat liver and HTC cells among various subcellular fractions are shown. Values are presented as percent of total counts in the cells. Errors are estimated to be $\pm 3\%$ of total counts.

	liver	HTC cells
cytoplasm (105 kg supernatant)	77%	56%
microsomes (105 kg pellet)	7%	20%
mitochondria (10 k g pellet)	16%	20%
nuclei and cell debris (400 g pellet)	<1%	4%

an active uptake of the drug by liver. We have not shown that nafenopin only enters the hepatocytes in the liver but there is evidence by Levine, etal, (1975) that much of the drug must enter the hepatocyte in order to explain the amounts of nafenopin secreted into the bile. This would suggest that the hepatocytes do actively sequester the drug and possibly shield other cells from its inhibitory effects. In addition, the hepatocytes also metabolize the drug to essentially deactivate the drug (Levine, etal, 1975; Handly, 1977). The bacteria probably escape the effects of nafenopin by metabolism as well, even though protein activity may not have increased.

There is some evidence for a hepatocyte stem cell in the liver which can be stimulated to divide and develop hepatocyte phenotype in response to a number of drugs (Inaoka, 1967; Grisham, 1980). These cells seem to be the terminal biliary duct cells. They do not have the same access to serum as the hepatocytes and therefore are not in contact with much of the drug.

The hepatocytes must have some way to signal the terminal biliary cells to divide. Koch and Leffert (1980) argue that the induction of hyperplasia involves a change in cell potential or an influx of Na^+ . This could be accomplished by electrical coupling between the cells or by the release of some factor into the blood stream from the hepatocytes. We find that the serum of rats after nafenopin administration does not contain a factor that will stimulate DNA synthesis in serum starved HTC cells. However, from this evidence alone, we cannot conclude that a serum factor

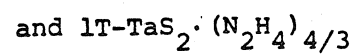
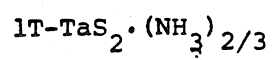
does not initiate mitosis in the stem cells.

An unforeseen result of this work is that phenoxyacetic acids (nafenopin is one of these compounds) now have been found to affect cell growth and metabolism in all phylogenetic kingdoms. 2,4-D, 2,4-dichlorophenoxyacetic acid, is well known as a plant growth regulator (Burstrom, 1950) and its herbicidal effects appear to be a result of abnormal growth of some cells and the termination of growth of others (Burstorm, 1950). Gamble (1975) proposed that these compounds act by altering the concentration of and disrupting the availability of ATP in plant and liver cells since the chemicals interact with a number of ATP dependent enzymes. We find that nafenopin inhibits growth in mammalian cells other than liver and in bacteria, too. Furthermore, nafenopin is found to inhibit the production of specific proteins of plasmid, bacterial and eukaryotic origin. Studies of the similarities in the synthesis of these proteins including pre- and post-translational processing are needed to determine how nafenopin effects this inhibition of a few proteins in such different species. It would be, indeed, intriguing to find all the affects of nafenopin and phenoxyacetic acids are secondary to disturbing the cells' energy supply.

- Benzce, W (1973) US 3,709,993
- Bucher, N and Malt, R (1971) Regeneration in Liver and Kidney,
Little, New York
- Burstrom, H (1950) Physiologia Pl, 3, 277
- Dulbecco, R and Vogt, M (1954) J Exp Med, 99, 167
- Gamble, W (1975) J Theor Biol, 54, 181
- Grisham, J (1980) Ann N Y Acad Sci, 349, 128
- Handly, N (1977) M. Sc. Thesis, Oxford University
- Inaoka, Y (1967) Gann, 58, 355
- Koch, K and Leffert, H (1980) Ann N Y Acad Sci, 349, 111
- Levine, W, Braunstein, I and Meijer, D (1975) Naunyn-Schmiedeberg's
Arch Exp Path Pharmacol, 290, 221
- Levine, W, Ord, M and Stocken, L (1977) Biochem Pharmacol,
26, 939
- Lowry, O, Rosebrough, N Farr, A and Randall, R (1951) J Biol Chem,
193, 265
- Maragoudakis, M (1969) J Biol Chem, 244, 5005
- Reddy, J, Svoboda, D and Azarnoff, D (1973) Biochem Biophys
Res Commun, 52, 537
- Reddy, M, Qureshi, S, Hollenberg, P and Reddy, J (1981)
J Cell Biol, 89, 406
- Schulte-Hermann, R (1974) Crit Rev Toxicol, 3, 97
- Waley, S (1974) Biochem J, 139, 789

Chapter 5

NMR study of



Introduction

TaS₂ is a member of a family of transition metal dichalcogenide compounds (TX₂), which are quasi-two dimensional solids exhibiting strong anisotropy of transport properties (e.g. conductivity) when measured parallel and perpendicular to the layers (Wilson, etal, 1975). The bulk phase is built of stacked layers and between each layer is a van der Waal's gap, a volume of weak interactions most likely due to the overlap of the chalcogen orbitals of adjacent layers.

Several different stacking patterns (crystal polytypes) can occur in TaS₂ and a number are illustrated in Figure 1. The 1T-TaS₂ polytype is especially interesting because of the presence of strong periodic lattice distortions or superlattices that distinguish several different phases between 150-400°K (Acrivos, 1979: Wilson, etal, 1975) wherein are noted distinct values for conductivity (DiSalvo, etal, 1973) and magnetic susceptibility (Wilson, etal, 1975).

1T-TaS₂ can react with a number of compounds such as amines which intercalate the van der Waal's gap and modify a number of the properties of the bulk phase.

Among the changes observed are the formation of the 3R polytype (Meyer, etal, 1975), an increase in the temperature of onset of superconductivity (Gamble, etal, 1971: Meyer, etal, 1975) and changes in phase behavior with temperature (Acrivos, 1979: Sarma, etal, 1982: Tatlock and Acrivos, 1978). Structural studies reveal that the formation of superlattices is also influenced by intercalation (Acrivos, 1979). How intercalation effects these changes is not clear, but some

evidence supports a charge transfer mechanism (Acrivos, 1979; Schöllhorn and Zagefka, 1977). Figure 2 summarizes some of the measurements of $1T-TaS_2$ reacted with hydrazine.

Nuclear magnetic resonance spectroscopy (NMR) and neutron diffraction offer another means for studying these intercalated solids. Both techniques have been used to probe the intercalant molecule and its micro-environment within the crystal, so far yielding information about the mobility of ammonia (Gamble and Silbernagel, 1975) and the geometries of ammonia (Gamble and Silbernagel, 1975) and pyridine (Bray and Sauer, 1972) in $2H-TaS_2$. Additional NMR evidence suggests that the ammonia molecule is sensitive to phase changes associated with superlattice formation in intercalated $2H-TaS_2$ (Silbernagel and Gamble, 1975).

The ability to study phase behavior in intercalated $1T-TaS_2$ at a microscopic level would greatly add to our understanding of these materials. This work reports NMR studies of $1T-TaS_2 \cdot (NH_3)_{2/3}$ and $1T-TaS_2 \cdot (N_2H_4)_{4/3}$ between 200-300°K.

Figure 1: Shown here are projections in the 1120 crystallographic plane of the crystal for three lattice types of TaS_2 . Open squares represent the metal sites and the open circles represent sulfur atoms. The solid horizontal lines locate the van der Waal's gap. In these three polytypes, the metal is octahedrally coordinated, trigonally coordinated or alternate layers of each in 1T, 2H and 4Hb, respectively.

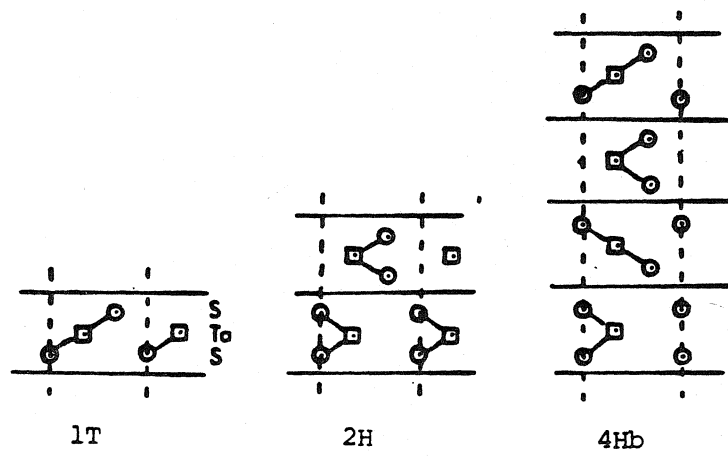
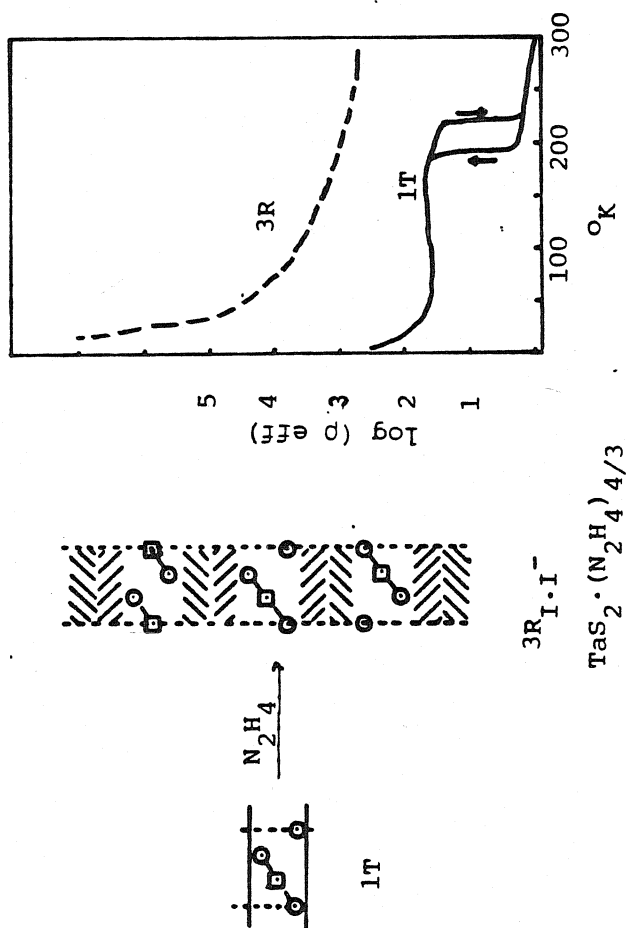


Figure 2: The 1T-TaS₂ lattice is shown here as a projection in the 1120 crystallographic plane for the virgin and hydrazine intercalated solid. Note that intercalation does not change the coordination of the metal atom in each layer, but does shift the position of the metal in adjacent layers to form the 3R_{I.I} polytype, so designated because two layers of hydrazine fill the van der Waal's gap. The ammonia intercalated solid, by contrast, forms the 3R_I polytype with only one layer of ammonia in the van der Waal's gap. Also shown in this Figure are the results of conductivity studies by Sarma, etal (1982) for the virgin 1T polytype and the hydrazine intercalated 3R_{I.I} polytype. The solid curve (—) is for 1T-TaS₂ and the dashed curve (----) is for 3R_{I.I} - TaS₂ · (N₂H₄)_{4/3}.



Methods

Samples

Crystals of $1T-TaS_2$ were gifts from Drs. T. Geballe of Stanford University and A. Beal of Cambridge University.

Intercalation

Crystals were placed in flattened NMR tubes to facilitate rotational studies and then connected to a vacuum line for intercalation. Ammonia and hydrazine were purified prior to exposure to the crystals. Ammonia was condensed on sodium to remove traces of water and then the gas was admitted to the sample. Hydrazine was distilled in situ and then admitted to the sample. Ammonia pressure was 700 Torr and hydrazine vapor pressure was 12 Torr. After one week at room temperature, the sample tube was immersed in liquid nitrogen and the tube sealed by melting the glass. This process could be completed without exposing the crystals to any condensed intercalant. Two samples were prepared with ammonia and one was prepared with hydrazine.

NMR Spectroscopy

Spectra were collected at 56.4 and 13.1 MHz. Free induction decays were collected for time averaging and then were Fourier transformed to give the absorption spectra. Temperature in the probe was varied by heating

nitrogen gas boiled from a dewar of liquid nitrogen.

With the system employed, temperature could be regulated within $\pm 0.5^{\circ}\text{K}$ of the desired value. A goniometer was mounted on the probe to assist the taking of spectra of samples at different angles with respect to the static magnetic field. Resonance frequency assignments were facilitated with the use of an acetyl chloride reference.

Results

Over the 200-300°K range there were three kinds of spectra for $1T-TaS_2 \cdot (NH_3)_{2/3}$ which define three temperature domains. Evidence of the three domains could be found in spectra of $1T-TaS_2 \cdot (N_2H_4)_{4/3}$ which were qualitatively the same as the spectra of ammonia intercalated $1T-TaS_2$.

Domain I 250-300°K

Two resonance lines were found. The resonance position of one was insensitive to crystal orientation in the magnetic field while the position of the other line was determined by the angle between the crystal c-axis and static magnetic field vector, H. The separation in frequency of the anisotropic and isotropic signals could be approximated by the equation:

$$\nu_a - \nu_i = A \cos^2 \theta$$

where ν_a and ν_i are line positions in Hz, A is the maximum separation in Hz and θ is the angle between the crystal c-axis and H. Shown in Figure 3 are plots of $\nu_a - \nu_i$, vs θ for ammonia and hydrazine intercalated samples. Table I presents A values for each.

The ratio of intensities of the anisotropic to isotropic NMR absorption (r_{ai}) was also a feature that characterized each temperature domain. In domain I, r_{ai} was a constant of the sample and not affected by

Table I

Values of A (maximum separation in Hz of the anisotropic and isotropic lines) for different temperatures are shown for all samples

	sample #1	sample #2	multiple lines				$T > 250^\circ \text{K}$	$T < 245^\circ \text{K}$
			530	300	130	110		
$1\text{T-TaS}_2 \cdot (\text{NH}_3)_2/3$			640					260
			500		90	-		360
$1\text{T-TaS}_2 \cdot (\text{N}_2\text{H}_4)_{4/3}$			200	-	-	-		55

Figure 3: Plots of $\nu_a - \nu_i$, the frequency of separation of the anisotropic from the isotropic line, in Hertz versus θ , the angle between the crystal c-axis and the magnetic field vector are presented in this Figure for $1T-TaS_2 (NH_3)_{2/3}$ (Sample #1) and $1T-TaS_2 (N_2H_4)_{4/3}$. Solid circles (●) show collected data with errors in frequency of ± 10 Hz and in angle of $\pm 3^\circ$. The solid curve appearing with the data is the plot of the $A \cos^2 \theta$ function where the A values are obtained from measurements of maximum observed separations (see Table I).

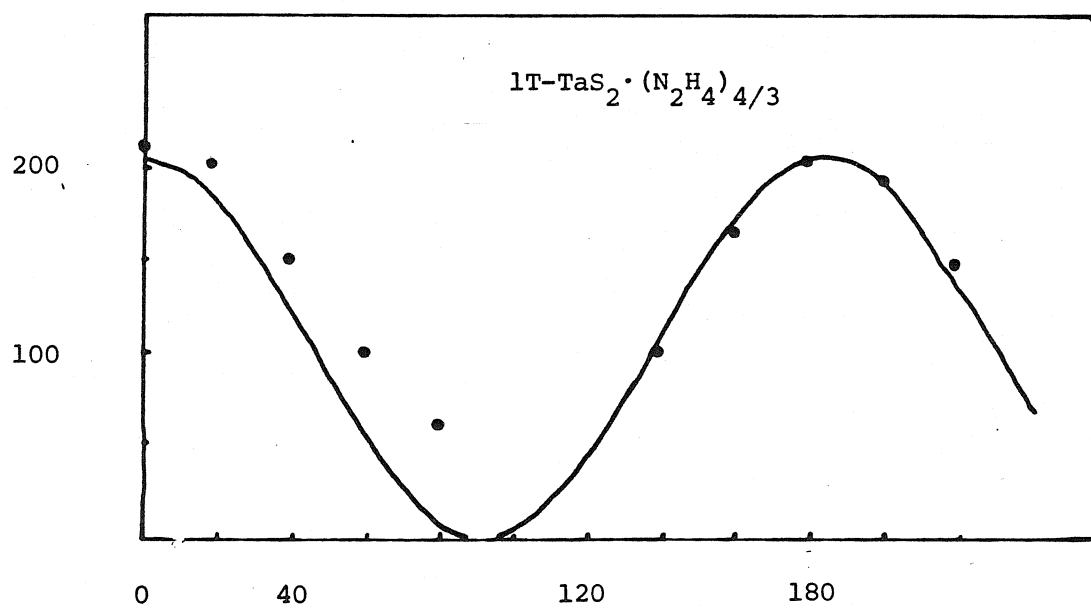
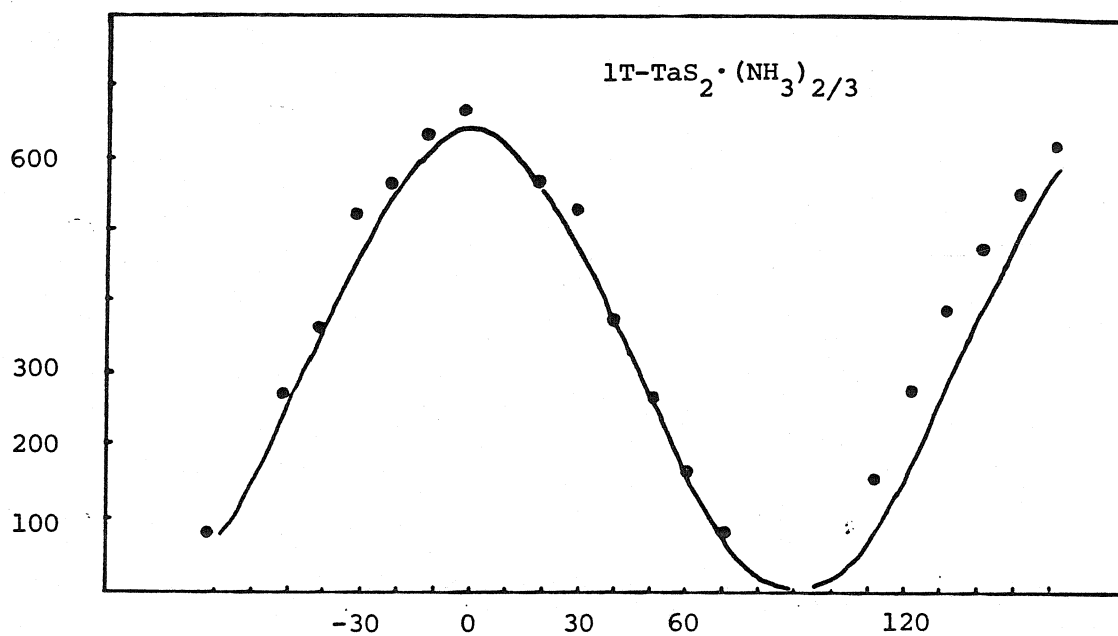
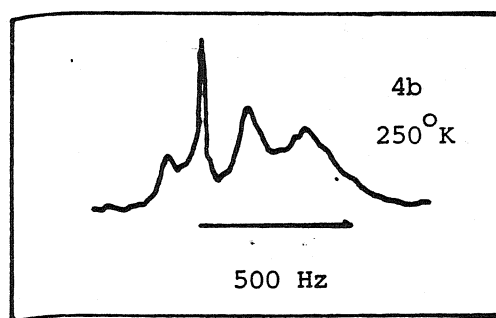
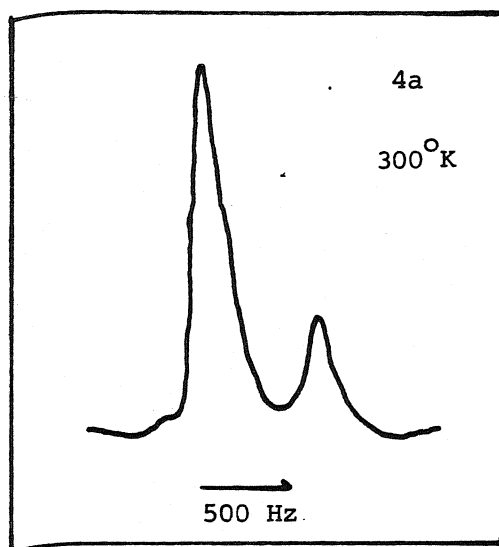


Figure 4a: In this figure is a representative spectrum of $1\text{T-TaS}_2 \cdot (\text{NH}_3)_{2/3}$ (sample #1) at room temperature and $\theta=0^\circ$. The anisotropic peak is at the right at higher frequency. The arrow is a 500Hz standard and points to higher frequency.

Figure 4b: This is a spectrum taken of $1\text{T-TaS}_2 \cdot (\text{NH}_3)_{2/3}$ (sample #1) at 250°K and $\theta=0^\circ$. The arrow is a 500Hz standard and points in the direction of increasing frequency. The isotropic peak is at the left.



variation of θ or temperature in this domain (data not shown).

Shown in Figure 4a is a representative spectrum of $1T-TaS_2 \cdot (NH_3)_{2/3}$.

Domain II $245^\circ - 250^\circ K$

In this range, spectra of $1T-TaS_2 \cdot (NH_3)_{2/3}$ were characterized by the presence of at least three lines; one isotropic and three or four anisotropic. For each of the anisotropic absorptions, the separation from the isotropic line followed the $A \cos^2 \theta$ behavior. A representative spectrum for $\theta = 0^\circ$ is shown in Figure 4b. When all the lines collapse at $\theta = 90^\circ$, the line width is equal to that of the isotropic line.

As was observed in domain I, the r_{ai} values for all anisotropic lines were constants of the sample (data not shown).

For $1T-TaS_2 \cdot (N_2H_4)_{4/3}$ there was an isotropic line and an unresolved manifold of several lines that collapsed at $\theta = 90^\circ$ and showed maximum separation at $\theta = 0^\circ$.





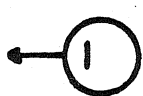
Domain III $200^\circ - 245^\circ K$

Between 200° and $245^\circ K$, there were two lines which showed the orientational dependence observed in domain I. However, there was a striking feature in this temperature domain which was not observed in domains I or II. Each time any samples were cooled, r_{ai} would take on

randomly two new values that would reversibly interconvert as the crystal was rotated through $\theta=90^\circ$ or $\theta=270^\circ$.

Figure 5 illustrates the change in r_{ai} upon rotation and contains pairs of r_{ai} values from several coolings.

Figure 5: This figure illustrates how rotation of a sample cooled to a temperature below 245°K can affect r_{ai} , the ratio of anisotropic to isotropic line intensity. A view down the instrument probe is shown to highlight the importance of the angle between the crystal c-axis and the magnetic field. The crystal is seen edge-on and is pictured in an exaggerated off axis position to help distinguish angles $\theta = 0^{\circ}$ and $\theta = 180^{\circ}$ which have different values of r_{ai} . The values of r_{ai} are shown for $1\text{T-TaS}_2 \cdot (\text{NH}_3)_{2/3}$ sample #1. The errors in measurement are estimated to be 10%.

$H_0 \rightarrow$		$r_{ai} \quad 1T-TaS_2 \cdot (NH_3)_{2/3}$				
		sample #1				sample #2
		a	b	c	d	
	0°	2.60	0.62	0.73	0.33	1.35
	45°					
	90°					
	135°					
	180°	2.29	0.27	0.89	2.41	1.88

Discussion

Our work shows that proton NMR of the guest molecules within TX_2 is a good probe of the micro-environments within intercalated complexes. Specifically, we find that the bulk phase predominantly determines the magnetic environment of the intercalants, NH_3 and N_2H_4 . Additionally, NMR reveals the presence of two micro-environments within the complexes as well as a phase transition at 245-250°K, most likely associated with the change in superlattice geometries observed in that temperature range by other methods (Acrivos, 1979; Tatlock and Acrivos, 1978).

Crystals intercalated with NH_3 and N_2H_4 both show the same two line pattern where the position of the low frequency peak is independent of and the high frequency peak is dependent upon the orientation of the crystal within the magnetic field. The proton line widths observed are consistent with a rapid re-orientation of NH_3 and N_2H_4 molecules within the layers. This is in agreement with the measurements made by Silbernagel and Gamble on $2\text{H-TaS}_2 \cdot (\text{NH}_3)$ (Gamble and Silbernagel, 1975).

Additionally, intercalant molecules do not appear to be able to exchange between the two magnetic environments that are the source of the isotropic and anisotropic peaks as there is no evidence of exchange broadening or averaging.

The presence of two spectral lines with different behaviors in the magnetic field suggests the presence of two micro-domains within the intercalated solid. We offer the following proposal for the identities of the magnetic environments leading to the two lines.

The isotropic signal arises from protons in fractured or poorly ordered domains and the anisotropic resonance is a result of protons occupying an ordered region where a superlattice is extant. Fractures and other crystal defects that would preclude superlattice formation have been observed by a number of investigators (Riekell and Schöllhorn, 1976 ; Tatlock and Acrivos, 1978), and the intercalation process itself may be responsible for some of these faults (Tatlock and Acrivos, 1978). Regardless of the cause of the crystal disorder, intercalant molecules in these disordered volumes would not be affected by fields oriented with the crystal geometry and, hence, give rise to the isotropic signal. Evidence for a role of superlattices in forming the anisotropic field is two-fold. First, Wilson, etal (1975), have measured bulk susceptibility in $1T-TaS_2$ and found variation of this parameter coincident with different superlattice geometries. Second, we find a complex, multi-line spectra with one line isotropic and the remainder anisotropic in the 235-240°K region. This is the same temperature range in which Acrivos (Acrivos, 1979 ; Tatlock and Acrivos, 1978) has observed a superlattice phase transition. In one of the materials we have studied, $1T-TaS_2 \cdot (N_2H_4)_{4/3}$, our spectra suggest that two or more distinct superlattices may be present within the sample in this temperature range as each superlattice would contribute a different susceptibility field and be revealed as distinct anisotropic lines.

Below 245°K, a two line (anisotropic and isotropic) signal like the room temperature spectra is found for $1T-TaS_2 \cdot (N_2H_4)_{4/3}$; however, a smaller separation between the two lines is observed. This suggests that a different superlattice occurs within these crystals in the 200-245°K range. Also, in this temperature range, a new pattern of resonance line intensity is observed. The sum of anisotropic and isotropic line intensities is not altered from that value observed at room temperature so the total number of protons in the sample remain constant within experimental uncertainty. Yet two discrete ratios of anisotropic to isotropic line intensities are found, one for each face of the crystal (See Figure 2), that do not change until the sample is warmed above 245°K. In addition, each cooling event yields a new pair of intensity ratios. The variation in intensities of the two peaks, which is not observed at temperatures above 245°K, presents an interesting problem. To account for this particular situation, we propose a mechanism whereby the formation of the superlattice at low temperature is affected by temperature. Each cooling would appear to lead to varying amounts of this superlattice since crystal defects may be locked in or introduced by the temperature change. As proposed for the origin of isotropic and anisotropic lines at high temperatures, the amount of the low temperature superlattice, and, hence, the anisotropic line intensity would be influenced by the volume of the crystal occupied by faults. While the temperature effects on relative line intensity are unpredictable, the effects of the magnetic field polarization

are not random. However, we are unable to explain this latter phenomenon.

Thus, we have shown that proton NMR studies of the intercalant molecule with an octahedrally coordinated TaS_2 host are able to describe the phase transition near 245°K which has not been observable by techniques based upon measurements of bulk properties. Additionally, our findings suggest that intercalants such as ammonia and hydrazine are sensitive to local magnetic fields caused by superlattices.

References

- Acrivos, J (1979) in Intercalated Layer Materials, ed. Levy, F
D. Reidel Publishing Co, Dordrecht, p33-98
- Bray, D and Sauer, E (1972) Solid State Commun., 11, 1239
- DiSalvo, F, Bagley, B, Voorhoeve, J and Waszczak, J (1973)
J. Phys. Chem. Solids, 34, 1957
- Gamble, F, Osiecki, J and DiSalvo, F (1971)
J. Chem. Phys., 55, 3525
- Gamble, F and Silbernagel, B (1975) J. Chem. Phys., 63, 2544
- Meyer, S, Howard, R, Stewart, G, Acrivos, J and Geballe, T
(1975) J. Chem. Phys., 62, 4411
- Riekell, C and Schöllhorn, R (1976) Mater Res Bull, 11, 369
- Sarma, M, Beal, A, Nulsen, S and Friend, R (1982)
J. Phys. C: Solid State Phys., 15, 477
- Schöllhorn, R and Zagefka, H-D (1977) Angew Chem Int Ed, 16, 199
- Silbernagel, B and Gamble, F (1974) Phys Rev Lett, 32, 1436
- Tatlock, G and Acrivos, J (1978) Phil Mag B, 33, 81
- Wilson, J, DiSalvo, F and Mahajan, S (1975) Adv Phys, 24, 117